A Serum- and Feeder-Free System to Generate CD4 and Regulatory T Cells from Human iPSCs

Authors

Helen Fong[1,2], Matthew Mendel[1], John Jascur[1,2], Laeya Najmi[1,3], Ken Kim[1], Garrett Lew[1], Swetha Garimalla[1,4], Suruchi Schock[1,5], Jing Hu[1], Andres Villegas[1], Anthony Conway[1,6], Jason D. Fontenot[1], Simona Zompi[1,7]

Classification: Original Research

Affiliation

[1] Sangamo Therapeutics, 501 Canal Blvd. Richmond, CA 94804

[2] Current affiliation: Proximity Therapeutics, 135 Mississippi Street, San Francisco, CA 94107

[3] Current affiliation: BioMarin, 105 Digital Dr, Novato, CA 94949

[4] Current affiliation: OmniAb, 5980 Horton Street, Suite 600 Emeryville, CA 9460

[5] Current affiliation: Radar Therapeutics, 2625 Durant Ave, Berkeley, CA 94720

[6] Current affiliation: Replay, 5555 Oberlin Drive, Unit 120, San Diego, CA 92121

[7] Current affiliation: Altos Labs, 1300 Island Drive, Redwood City, CA 94065

Corresponding authors

Matthew Mendel: mmendel@sangamo.com

Helen Fong: hfong82@gmail.com

Simona Zompì: simona.zompi@gmail.com

Abstract

iPSCs can serve as a renewable source of a consistent edited cell product, overcoming limitations of primary cells. While feeder-free generation of clinical grade iPSC-derived CD8 T cells has been achieved, differentiation of iPSC-derived CD4sp and regulatory T cells requires mouse stromal cells in an artificial thymic organoid. Here we report a serum- and feeder-free differentiation process suitable for large-scale production. Using an optimized concentration of PMA/Ionomycin, we generated iPSC-CD4sp T cells at high efficiency and converted them to Tregs using TGFβ and ATRA. Using genetic engineering, we demonstrated high, non-viral, targeted integration of an HLA-A2 CAR in iPSCs. iPSC-Tregs +/- HLA-A2-targeted CAR phenotypically, transcriptionally and functionally resemble primary Tregs and suppress T cell proliferation *in vitro*. Our work is the first to demonstrate an iPSC-based platform amenable to manufacturing CD4 T cells to complement iPSC-CD8 oncology products and functional iPSC-Tregs to deliver Treg cell therapies at scale.

Introduction

Engineered autologous T cell therapies have shown the ability to transform the oncology field, yet producing these products at scale for large numbers of patients has proven challenging. The ability to derive hypoimmunogenic engineered T cells from self-renewing human induced pluripotent stem cells (iPSCs) could significantly increase access to these therapies[1-3]. The advantages of using iPSCs over primary cells include the capacity to easily multiplex edit the starting cell source, access to a self-renewable and well-characterized product, and standardization of the product through the development of a master cell bank (MCB). However, while using iPSCs as source material can have numerous benefits in terms of standardization and scale-up, differentiation of T cells from iPSCs has been challenging.

Access to a self-renewable, potentially unlimited source of cells is particularly attractive for cell types that are difficult to isolate or present in small numbers, such as regulatory T cells (Tregs). In recent years there has been much interest in the use of Tregs to treat a wide variety of diseases, including autoimmune disorders, as well as in organ transplantation[4]. As of 2022, there were more than 30 active and completed clinical trials evaluating the safety and efficacy of Treg cell therapies[5]. Most of the studies have focused on *in vitro*-expanded polyclonal Tregs but showing limited clinical efficacy. Promising preclinical results testing antigen-specific CAR Tregs[6] led to the first CAR Treg clinical trial authorization (NCT04817774) for kidney transplant patients, using *ex vivo,* autologous, naïve Tregs engineered with a CAR construct recognizing HLA-A2, to investigate the induction of tolerance in HLA-A2 negative patients receiving an HLA-A2 positive renal graft.

Currently, sourcing $CD4^+$ T cells and Tregs for cell therapies is invasive, time-consuming, and yields small numbers, particularly of Tregs which comprise only 5-7% of the circulating CD4 T cell population[7]. Furthermore, $CD4^+$ T cells and Tregs obtained from these sources are polyclonal in

60 nature and can introduce variability and non-specificity. While we have been successful in
61 introducing a CAR construct in primary Tregs to mediate a specific immunosuppressive
62 response[6], a process for generating specific $CD4^+$ T cells and Tregs, especially genetically
63 engineered cells, with high efficiency and at clinically relevant scale has remained a challenge.
64
65 Numerous studies have shown the ability to generate large quantities of T cells from iPSCs,
66 focusing primarily on the differentiation to cytotoxic T lymphocytes (CTLs)[8-10]. Improvements have
67 recently been made in the differentiation processes to generate iPSC-derived CAR CD8 single
68 positive (CD8sp) T cells that more closely resemble primary $CD8\alpha\beta^+$ T cells rather than innate $\gamma\delta$
69 T cells, by knocking out *TRAC* and delaying and attenuating CAR expression[11, 12]. The artificial
70 thymic organoid (ATO) system has also proven to be successful in generating functional
71 $CD3^+CD8\alpha\beta^+$ T cells that produce IFN-γ, TNF-α, and IL-2 and proliferate upon stimulation[10].
72 Recent data from the Human Cell Atlas group reported that these CD8 T cells differentiated *in*
73 *vitro* were most similar to type 1 innate T cells - a prenatal unconventional T cell type particularly
74 abundant during early development in the fetus that expresses high levels of *ZBTB16*
75 (Promyelocytic Leukemia Zinc Finger Protein or PLZF) and has an innate-like transcriptional
76 profile[13]. The authors further hypothesize that unconventional T cells arise *via* thymocyte-
77 thymocyte (T-T) interactions during development as well as in the ATO system which does not
78 contain any thymic epithelial cells (TECs)[13].
79
80 Interestingly, the ATO system also produces a small population of $CD3^+CD4^+$ T cells[10, 14] that can
81 be converted to $FOXP3^+$ Tregs[15]. However, a scalable method to generate clinically relevant
82 numbers of $CD4^+$ T cells and Tregs from iPSCs has yet to be demonstrated. This need has
83 become more compelling in recent years as $CD4^+$ T cells are known to enhance $CD8^+$ CTL

84 responses[16] and have been shown to be therapeutically useful in CAR-T cell therapies, increasing
85 product potency[17, 18] and demonstrating long-term functional persistency in clinical trials[19].
86 Current methods to generate CD8sp T cells, CD4 single positive (CD4sp) T cells and Tregs from
87 iPSCs utilize serum or mouse stromal cells at some stage of the differentiation process making it
88 difficult for use in clinical development. In addition, the use of an ATO system is challenging to
89 scale-up for manufacturing as it requires the maintenance of a 3D system and involves
90 dissociation and extraction of the cells of interest from a mixed population of mouse and human
91 cells. Here we show for the first time the ability to efficiently generate both CD4sp T cells and
92 Tregs from iPSCs in completely serum- and feeder-free conditions. We identified a potent cell
93 stimulator to convert $CD4^+CD8^+$ double positive T (DP T) cells to CD4sp T cells at high efficiency
94 that can be further converted to $FOXP3^+$ Tregs using TGFβ, all-trans retinoic acid (ATRA), and
95 IL-2 with CD3/CD28/CD2 activation. We show that the iPSC-CD4sp T cells have an innate-like
96 transcriptional profile, including *ZBTB16* expression, evocative of prenatal unconventional T
97 cells[13], can be activated upon stimulation and secrete IL-2 and IL-4. The iPSC-Tregs possess
98 typical Treg characteristics, are transcriptionally more similar to primary Tregs than primary
99 conventional T (Tconv) cells and suppress primary CD4 Tconv proliferation. In addition, iPSCs
100 engineered to express an HLA-A2 CAR and a fully functional TCR under the control of the *TRAC*
101 promoter could effectively differentiate to CD4sp T cells and Tregs that suppress Tconv
102 proliferation *via* activation through the TCR or the HLA-A2 CAR. Finally, we show that the iPSC-
103 Tregs are amenable to cryopreservation and retain function post-thaw. This novel method
104 provides a viable path forward towards the development of a scalable iPSC-derived Treg cell
105 therapy for autoimmune diseases. This novel process provides a high yield of innate-like iPSC-
106 CD4sp cells. Further optimization of culture media composition and/or cell engineering
107 approaches should achieve a fully mature iPSC-derived CD4sp T cells which could enhance the
108 iPSC-derived CD8sp T cell products currently in the clinic for oncology applications[17, 19, 20].

Results

Generation of CD34$^+$ hematopoietic stem and progenitor cells (HSPCs) and T cell progenitors from iPSCs

iPSCs were derived from sorted CD4$^+$CD25$^+$ cells from a healthy human donor. Derivation of iPSCs from T cells has been previously documented with resulting T cells differentiated from reprogrammed iPSCs possessing antigen specificity due to retention of a rearranged TCR[9, 21, 22]. Additionally, evidence suggests improved T cell lineage differentiation when iPSCs originate from mature T cells due to removal of the barrier to TCR rearrangement[9, 23]. CD4$^+$CD25$^+$ T cells were isolated and FACS-purified from healthy human leukapheresis blood and reprogrammed by Sendai virus carrying vectors encoding for the four Yamanaka factors: OCT-4, SOX2, KLF4, and C-MYC. Multiple clones were generated and characterized by immunocytochemistry to confirm expression of OCT4, SOX2, TRA-1-81, and SSEA-4 **(Supp. Figure 1A)**. Pluripotency was confirmed using the PluriTest assay (ThermoFisher, **Supp. Figure 1B**). In addition, G-band karyotyping confirmed the absence of any chromosomal aberrations **(Supp. Figure 1C)**.

To facilitate future translation from discovery to process development we utilized serum-free, commercially available reagents from the iPSC stage to the DP T stage. As a first step, a modified version of the spin embryoid body (EB) method was used to differentiate the iPSCs into early stages of hematopoiesis from days 0 to 8, followed by expansion of the hematopoietic stem and progenitor cells from days 8 to 14[24, 25] **(Figure 1A)**. The EBs increased in size over time and by day 14, numerous free-floating HSPCs emerged around the periphery expressing both CD34 and CD45 (65%±13.5%, n=3) **(Figure 1B and 1C)**. The approximate yield of HSPCs per input iPSC was 16.5±9.3, n=3 **(Figure 2)**.

For commitment and differentiation to the T cell lineage, interaction between blood cell progenitors and a Notch ligand is required[26-28]. To differentiate the iPSC-HSPCs to lymphoid progenitors, the

133 entire population of free-floating HSPCs was separated from the EBs, collected, and seeded onto
134 plates coated with lymphoid differentiation coating material (LDCM), a commercially available
135 matrix containing a Notch ligand **(Figure 1D)**. The HSPCs were then further differentiated to
136 lymphoid progenitor cells that were CD5 and CD7 DP by day 28 (**Figure 1C**, 67.4±0.1%, n=6)
137 and subsequently to CD4 and CD8 DP T cells by day 42 (**Figure 1C**, DP T cells, 86.3±0.1%, n=5)
138 using a commercially available iPSC-HSPC to T cell differentiation system **(Figure 1D)**. The
139 approximate yield of lymphoid progenitor cells and DP T cells was 2.3e3±1.4e3 per input iPSC
140 and 2.6e4±1.6e4 per input iPSC, respectively **(Figure 2)**. We tested the use of CXCL12 (SDF1a)
141 and a p38 inhibitor (SB203580) to enhance the number of DP T cells[22] and found an approximately
142 1.8-fold increase in DP T cells **(Supp. Figure 2)**.

143 **Generation of CD4-sp T cells and FOXP3$^+$ Tregs from iPSC-CD4$^+$CD8$^+$ DP T cells**

144 During T cell development in the thymus, TCR signaling is required in DP thymocytes to induce
145 positive selection and subsequent generation of either mature CD4$^+$ or CD8$^+$ T cells[29]. In addition
146 to differentiation into T cells, the interaction between the TCR and MHC molecules in the thymus
147 also rescues thymocytes from programmed cell death[30]. Alternatively, it has been shown that DP
148 thymocytes can undergo positive selection and maturation into CD4$^+$ T cells without engagement
149 of the TCR if provided with a strong, persistent signal[29, 31, 32]. We tested the ability of the iPSC-
150 derived DP T cells (iPSC-DP T) to convert to CD4sp T cells by exposure to three different doses
151 (low, medium, high) of the potent cell stimulator PMA/Ionomycin (PMA/I) **(Figure 3A).** A change
152 in phenotype was observed by 24 hours when the iPSC-DP T cells appeared to be primarily
153 CD8sp initially but shifted dramatically to become CD4sp 4 days after treatment. After 6 days,
154 more than 50% of the cells were CD4sp at the lowest concentration of PMA/I **(Figure 3B)**. Medium
155 to high concentrations of PMA/I were also effective in converting iPSC-DP T cells to CD4sp T
156 cells albeit at lower efficiency (**Supp. Figure 3**). The cells remained DP in the absence of PMA/I.
157 Commitment to the CD4 lineage is typically specified by the zinc-finger transcription factor and

master regulator ThPOK [33]. At the lowest concentration of PMA/I, ThPOK could be observed in the $CD3^+TCR\alpha\beta^+CD4^+$ population of developing T cells **(Figure 3C)**. Without PMA/I stimulation, the DP T cells did not progress towards the CD4 lineage and the minor population of $CD4^+$ cells did not express ThPOK. The yield of CD4sp cells from PMA/I treated iPSC-DP T cells was approximately 4.3e3±2.3e3/input iPSCs **(Figure 2)**. The generated iPSC-CD4sp cells expressed $CD45RO^+$, but not CD45RA, and highly expressed the co-receptor CD28. CD62L was expressed at low levels compared to primary Tconv (**Figure 3D** and **Supp. Figure 4**).

After successfully generating CD4sp T cells from iPSCs, we next interrogated whether a regulatory phenotype could be induced to produce Tregs. Previous studies have shown the ability to generate $FOXP3^+$ Tregs from $CD4^+CD25^-$ T cells, termed induced Tregs (iTregs), in the presence of TGFβ and IL-2[34, 35 36]. To determine if the iPSC-CD4sp T cells could also be induced to express FOXP3, cells were treated with a commercially available cocktail of TGFβ, all-trans retinoic acid (ATRA), and IL-2 and supplemented with a soluble T cell activator composed of anti-human CD3, CD28, and CD2 monospecific antibody complexes on day 50 of differentiation **(Figure 3A)**. Seven days post-treatment (day 57) with the TGFβ cocktail and soluble activator, an increase in frequency of DN and CD8sp T cells was observed and, while reduced, the culture retained a sizeable CD4sp T cell population **(Figure 3E)**. When gating on the CD4sp T cell population the cells expressed CD25, low levels of CD127 and high levels of FOXP3 similar to primary Tregs. Approximately 26% (+/-9.2%; n=6) of the total live population displayed a ≥90% CD4spCD25CD127lowFOXP3$^+$ phenotype. In addition, the CD4sp T cell population maintained expression of ThPOK while co-expressing FOXP3 **(Figure 3E)**. We observed an average yield of 5.9e3±4.4e3 (n=3) iPSC-Treg/input iPSC **(Figure 2)**.

iPSC-CD4sp T cells displayed a molecular signature similar to that of unconventional T cells while iPSC-Tregs displayed a molecular signature similar to that of primary Tregs

182 As the populations of iPSC-CD4sp cells and iPSC-Tregs are heterogenous post-PMA/I and post-
183 TGFβ and ATRA treatment, we sought to isolate the CD4sp population at day 50 and the target
184 Treg population of CD4spCD25^{+}CD127^{-}FOXP3^{+} iPSC-Tregs at day 57 by FACS to further
185 characterize them by single-cell RNA sequencing (scRNA-seq). For iPSC-Tregs, a population of
186 target cells that is >90% FOXP3 was obtained by gating on a "CD25 high" population from the
187 total population of live, single CD4sp T cells **(Supp. Figure 5)**.

188 To determine the similarity between the iPSC-CD4sp to primary CD4 T cells and the iPSC-Tregs
189 to primary Tregs, their transcriptomes were compared. Five cell samples were analyzed: (1)
190 sorted iPSC-Tregs; (2) primary Tregs; (3) induced Tregs (generated from primary naïve CD4 T
191 cells); (4) iPSC-CD4sp; and (5) primary CD4 Tconvs. A global comparison of differentially
192 expressed genes within the 5 samples by hierarchical clustering revealed that iPSC-CD4sp T
193 cells were similar in their transcriptional profile to primary Tconv while primary Tregs were similar
194 to induced Tregs. The iPSC-Tregs however, were distinct in their gene expression profile **(Figure
195 4A).** Using Cell Typist and the Human Cell Atlas public data[13, 37, 38] to predict and automatically
196 annotate scRNAseq data, we show that the cells in all five samples were classified as T cells with
197 high probability (**Supp. Figure 6A**). In addition, a large majority of primary Tregs & iPSC-Tregs
198 were declared as Tregs by CellTypist when compared to either adult or fetal cell types (**Supp.
199 Figure 6B and 6C**). The iPSC-CD4sp were more similar to type 3 innate lymphoid (ILC3) cells
200 when compared to adult immune cells (**Supp. Figure 6B**) and were not able to be classified when
201 compared to fetal immune cells (**Supp. Figure 6C**). The lower transcripts in the iPSC-CD4sp
202 population compared to primary CD4 T cells may (**Supp. Figure 6D**) explain the difficulty in
203 classifying these cells using Cell Typist. An analyses of marker genes across developmental
204 stages and cell types shows that both iPSC-Tregs and iPSC-CD4sp display a more immature
205 phenotype as compared to their primary adult counterparts **(Figure 4B)**. In addition, iPSC-CD4sp
206 express genes that are found in innate immune cells and in unconventional fetal T cells, in

particular a marked expression of *ZBTB16* (PLZF) found in fetal unconventional T cells and innate cells **(Figure 4B** and **Supp. Figure 6D)**.

A visualization of cells by cluster for the iPSC-Tregs, cultured primary Tconv (CD4sp), cultured primary Treg and induced Tregs was performed using UMAPs (**Figure 4C**). Known markers of Tregs and their segregation among the clusters was explored. All clusters express *CD4* but express low to no levels of *CD8*. All clusters express *IL2RA* (CD25) with particularly strong expression in induced Tregs. *FOXP3* expression was strongest in sorted iPSC-Tregs followed by primary cultured Tregs and induced Tregs in contrast to Tconvs which do not express high levels of *FOXP3*. Both sorted iPSC-Tregs and primary Tregs express higher levels of *IKZF2* (Helios) than primary Tconv and induced Tregs. *IL7R* (CD127) is highly expressed in primary Tconv with mid- to low-level expression in all other clusters. We sought a more refined analysis and examined the expression of a core Treg gene signature in all samples[39, 40 41] **(Figure 4D)**. We found that the iPSC-Tregs were similar to primary Tregs and induced Tregs with some differences in gene expression. The iPSC-Tregs had upregulated expression of *FOXP3 and CTLA4* and downregulated expression of *TNFRSF1B*.

Characterization and functional assessment of iPSC-CD4sp T cells and iPSC-Tregs

Further characterization and functional assessment were performed on sorted iPSC-CD4sp T cells and compared to their primary Tconv counterpart. iPSC-CD4sp T cells were activated with CD3/CD28/CD2 soluble activator. After activation, cells increased their expression of activation markers CD25 and PD-1 at 24 hours **(Supp. Figure 7A and Supp. Figure 7B)** and at 48 hours **(Figure 5A and Figure 5B)** while decreasing expression of CD28 similar to Tconv **(Supp. Figure 7B and Figure 5B)**. While CD69 MFI increased after activation, the frequency of cells expressing CD69 did not change. Activated iPSC-CD4sp T cells also secreted pro-inflammatory cytokines IL-2 and TNF-α similar to activated primary Tconv but did not secrete IFN-γ. Similar levels of IL-4

231 and IL-10 were secreted by iPSC-CD4sp T cells compared to primary Tconv after stimulation
232 **(Figure 5C).**

233 We then characterized and examined the *in vitro* function of sorted iPSC-Tregs.
234 Immunophenotyping of cells post-sort showed a typical Treg phenotype with an average of
235 83.4±6.3% FOXP3 expression (n=5) and average 91.6±1.6% Helios expression (n=2) from total
236 live cells. Demethylation of the evolutionarily conserved non-coding element FOXP3 Treg-
237 specific demethylated region (FOXP3 TSDR) is required for stable FOXP3 expression in Tregs[42].
238 It is typically methylated in Tconv, induced Tregs and other non-Treg blood cells[43]. We examined
239 the methylation state of FOXP3 TSDR by high resolution melt quantitative polymerase chain
240 reaction (HRM-qPCR) in the sorted iPSC-Tregs. The iPSC-Tregs demonstrated >90%
241 demethylation similar to the primary Treg positive control. In contrast, primary $CD4^{+}CD25^{-}$ Tconv
242 as well iPSC-CD4sp T cells were highly methylated at FOXP3 TSDR **(Figure 5D)**. The sorted
243 iPSC-Tregs could be activated via their TCR using beads coupled to anti-CD3 and anti-CD28
244 antibodies (Dynabeads). After activation, the iPSC-Tregs increased the expression of early
245 activation marker CD69 on average of 3-fold with no change to their Treg phenotype **(Figure 5E-**
246 **F)**.

247 Tregs typically exert their suppressive function through various mechanisms including
248 suppression by cytolysis[44, 45]. Cellular toxicity was determined by co-culturing activated and
249 unactivated iPSC-Tregs with primary CD4 Tconv target cells. Compared to activated cytotoxic
250 primary CD8 T cells, activated iPSC-Tregs had low cytolytic activity similar to activated primary
251 Tregs as measured by LDH release assay **(Figure 6A).**

252 Additional suppressive mechanisms include secretion of anti-inflammatory cytokines like IL-10[44].
253 IL-10 is produced by a variety of cells including $CD4^{+}$ Th2 cells, Tregs and IL-10-induced $CD4^{+}$ T
254 reg cells (Tr1 cells)[46]. Interestingly, iPSC-Tregs express higher, but variable, amounts of IL-10 as

compared to primary Tregs. Importantly, the iPSC-Tregs secreted low levels of pro-inflammatory cytokines IL-2, IFN-γ, and TNF-α before and after activation, similar to primary Tregs **(Figure 6B)**.

The cardinal feature of Tregs is their ability to suppress the activation and proliferation of Tconv or Teff cells by a cell-to-cell contact mechanism[44]. To determine the suppressive function of activated iPSC-Tregs, the cells were co-cultured with activated primary Tconv and their proliferation was measured by flow cytometric analysis. Activated iPSC-Tregs effectively suppressed Tconv proliferation at a 1:1 ratio of Tregs:Tconv similar to activated primary Tregs **(Figure 6C)**. Without activation, iPSC-Tregs had significantly lower levels of suppression at 1:1 to 1:4 Tregs: Tconv ratios. An iPSC-Treg dose-dependent effect on Tconv suppression was also observed similar to primary Tregs. As expected, when iPSC-CD4sp T cells were tested for suppressive function, they were unable to prevent Tconv proliferation even at the highest ratio of 1:1 CD4sp T cells:Tconv **(Figure 6C)**. This confirms that the suppressive function is specific to iPSC-Tregs and appears only after conversion of iPSC-CD4sp T cells to FOXP3$^+$ Tregs and after cell activation.

Generation and functional assessment of HLA-A2 CAR$^+$ iPSC-Tregs

We next investigated the function of iPSC-Tregs equipped with a chimeric antigen receptor (CAR). To this end, we genetically engineered iPSCs to express an HLA-A2 CAR using zinc-finger nucleases (ZFNs) targeting exon 2 of the *TRAC* gene.

We sought to retain expression of the *TRAC* gene and utilized a donor sequence comprised of *TRAC* cDNA encompassing the *TRAC* exonic sequence downstream of the integration site. This donor sequence is placed upstream and in-frame with a T2A coding sequence such that the engineered locus retains expression of the TCRα chain while expressing an HLA-A2 CAR under the control of the *TRAC* promoter **(Figure 7A)**. Through optimized electroporation of the iPSCs

278 with TRAC ZFN mRNA and donor DNA we achieved a >80% targeted integration without selection
279 as assessed by sequencing of the bulk edited population.

280 The resulting engineered iPSCs were cloned, expanded, and sequenced to obtain a biallelically
281 modified iPSC clone with the HLA-A2 CAR inserted at the target site. Sequencing analysis
282 confirmed the precise and in-frame insertion of a single copy of donor DNA (HLA-A2-CAR),
283 without any detected mutations. The CAR-engineered iPSCs also displayed a normal pluripotent
284 phenotype and were karyotypically normal **(Supp. Figure 1)**. To generate HLA-A2 CAR$^+$ iPSC-
285 Tregs (CAR iPSC-Tregs) the iPSCs were differentiated to HSPCs, lymphoid progenitor cells, and
286 DP T cells using the same differentiation process utilized for unedited iPSCs as described above
287 **(Supp. Figure 8A)**. HLA-A2 CAR iPSCs could also generate CD4sp T cells and FOXP3$^+$ Tregs
288 **(Supp. Figure 8B, 8C)**. Of note, we observed a 2.2-fold lower yield of Tregs (n=3, ±0.2 fold) from
289 the HLA-A2 CAR iPSCs compared to Tregs generated from unedited iPSCs. By flow cytometric
290 analysis, we found that ~90% (90.1%±1.8%, n=4) of the DP T cells were already expressing the
291 CAR by day 42 and retained high CAR expression at both the CD4sp T cell (99%±0.2%, n=4) and
292 Treg stages (99.85%±0.1%, n=4). The intensity of CAR expression increased as the cells
293 differentiated as measured by MFI **(Supp. Figure 8D)**.

294 Similar to unedited iPSC-Tregs, HLA-A2 CAR$^+$ iPSC-Tregs could also be sorted. Four days post-
295 sort the expression levels of the CAR remained stable (81.3±12.4% of TCRαβ$^+$ cells and
296 MFI=9814.3±1143.3, n=3) and the cells maintained a high level of demethylation at FOXP3 TSDR
297 (88%±10.3%; n=3).

298 Further characterization showed that the CAR iPSC-Tregs could be activated through both the
299 TCR and the HLA-A2 CAR demonstrating the engineering strategy successfully retained TRAC
300 expression while integrating a functional CAR. Activation of the CAR iPSC-Tregs using either
301 CD3/CD28 beads (Dynabeads) or HLA-A2 dextramer (as previously described[6]) upregulated
302 CD69 expression compared to unactivated or dextramer control activation **(Supp. Figure 9A,**

9B). TCR- and CAR-mediated activation induced a very low level of pro-inflammatory cytokines while inducing higher levels of IL-10 **(Supp. Figure 9C)** similar to levels of cytokines produced by unedited iPSC-Treg upon TCR activation **(Figure 6B).** The CAR iPSC-Tregs significantly suppress Tconv proliferation at similar levels to wild-type iPSC-Tregs when activated either through the TCR or the HLA-A2 CAR, while unactivated or control dextramer activated CAR iPSC-Tregs only displayed a basal level of suppression **(Figure 7B).**

Characterization and functional assessment of cryopreserved CAR iPSC-Tregs

A requirement for a viable CAR iPSC-Treg therapy is the ability to efficiently cryopreserve and store the cells for future use without loss of stability and function. Towards that goal, we cryopreserved iPSC-Tregs post-sort and then thawed, characterized, and tested their suppressive function. Approximately 80% of cells were recovered post-thaw (avg=82.5%, n=2) with a viability comparable to pre-cryopreservation (avg=74%, n=2). The CAR iPSC-Tregs maintained their phenotype post-thaw **(Supp. Figure 10A)**. The cells were also highly demethylated at FOXP3 TSDR (95.5±0.5%, n=2) and displayed an average 4-fold increase in CD69 after activation *via* the HLA-A2 CAR **(Supp. Figure 10B).** Finally, thawed CAR iPSC-Tregs were able to suppress Tconv proliferation when activated *via* the TCR or CAR **(Figure 7C).**

319 ## Discussion

320 We report here for the first time a serum- and feeder-free method to produce CD4sp T cells and
321 functional Tregs with and without a CAR from iPSCs. While the generation of CD4sp T cells from
322 iPSCs has been reported[10, 14], it currently requires the use of murine stromal cells and animal
323 serum (fetal bovine serum, FBS) in ATOs. The use of xenogenic feeders, animal serum and 3D
324 organoids is not ideal for the development of a clinical-grade therapeutic product. This is due to
325 issues with safety, scalability and serum batch-to-batch heterogeneity as well as difficulty
326 dissociating cells from 3D organoids. In addition, automation of 3D organoid generation to
327 produce large-scale reproducible organoids is a nascent field and will require further optimization
328 to minimize variability across differentiation batches[47]. The method proposed here circumvents
329 many of these issues and increases its amenability for manufacturing cell therapies at scale.

330 The reprogramming of T cells to pluripotency and subsequent differentiation to mature T cells has
331 been well documented particularly towards the generation of CD8$\alpha\beta^+$ CTLs[48, 49 50]. Using T cell-
332 derived iPSCs may aid in more efficiently generating iPSC-T cells as the early stages of T cell
333 development that are characterized by failed TCR rearrangement and cell death are bypassed[51].
334 While antigen specificity is unknown, reprogramming from a T cell clone possessing a single
335 TCR[9, 21, 52] or introducing a CAR or transgenic TCR at the iPSC or T cell stage[8, 11, 12, 22, 53, 54] can
336 help confer specificity. Based on these findings, we sought to utilize a similar strategy to develop
337 CD4sp T cells and Tregs from iPSCs. We were able to successfully obtain iPSCs from mature
338 CD4sp T cells that expressed classic pluripotency markers and appeared as compact colonies
339 with well-defined borders. The iPSCs were amenable to genome engineering for the targeted
340 integration of an HLA-A2 CAR. Both the wild-type and engineered iPSC lines were karyotypically
341 normal **(Supp. Figure 1)**. We did not perform deep characterization of off-targets in edited iPSCs
342 at this research-grade stage. Most importantly, an advantage of using iPSCs over primary cells is

343 the ability to select through whole-genome sequencing (WGS) well-characterized clones with no
344 specific off-targets and expand them to generate a MCB for future clinical use.

345 Methods to differentiate iPSCs into HSPCs and progenitor T cells are readily available, but many
346 require the combination of multiple individual reagents from various sources which may contribute
347 to increased variability in differentiation. We found that utilizing commercially available reagents
348 specifically designed to generate HSPCs and T cell progenitors from iPSCs streamlined the
349 differentiation process while satisfying the serum- and feeder-free requirements. We utilized a
350 modified EB-based method to differentiate iPSCs and employed commercially available serum-
351 free media for the generation of $CD34^+CD45^+$ HSPCs capable of differentiation to lymphoid cells.
352 It is worth noting that while the process yielded a mixture of $CD34^+$ and $CD34^-$ cells, no enrichment
353 or purification for $CD34^+CD45^+$ target cells was required for further differentiation. Indeed, we
354 found that by separation of the free-floating progenitor cells from the main EB we were able to
355 generate lymphoid progenitor cells that co-expressed CD5 and CD7 marking their T cell
356 commitment[55, 56]. Continued differentiation of the lymphoid progenitor cells resulted in CD4 and
357 CD8 DP T cells again, without enrichment of the starting population.

358 Thymic DP T cells express both CD4 and CD8 co-receptors that promote TCR engagement of
359 MHC ligands to enhance signal transduction[29]. Through various strengths of binding affinity to
360 MHC ligands, the developing T cells will undergo positive selection to survive or cell death by
361 negative selection[57]. The step-by-step natural process followed by DP T cells after positive
362 selection to commit to either the CD4sp or CD8sp lineage is unclear[29, 58]. It has been suggested
363 that a persistent and potentially stronger TCR signal is required to make the CD4 choice and block
364 re-expression of the CD8 co-receptor. To mimic the signal required for positive selection and
365 commitment to the CD4 lineage at the DP T cell stage, we utilized a strategy previously shown to
366 induce CD4 commitment in murine DP T thymocytes without TCR engagement[31]. The addition of
367 PMA/I activates protein kinase C and elevates calcium levels, respectively and in a similar manner

368 to TCR-mediated activation with signals from co-stimulator molecules like CD4, CD8 and LFA-1,
369 by-passing TCR engagement[31, 59]. At levels between 0.016 μM to 0.16 μM of PMA and 0.13 μM
370 of ionomycin, TRAC KO murine DP T thymocytes are positively selected to CD4 T cells. Higher
371 concentrations of PMA/I (1.6 μM and 1.3 μM, respectively) were inefficient in generating CD4 T
372 cells. These findings are consistent with our method in that the lower concentrations we used
373 successfully converted cells to the CD4 lineage while higher concentrations of PMA/I were less
374 efficient. Importantly, after conversion to CD4sp T cells, ThPOK expression was observed further
375 confirming its lineage commitment (**Figure 3C**). The kinetics of co-receptor expression in our
376 system is different from what has been previously published in mouse-derived thymocytes[31, 59, 60]
377 and could be due to species-specific differences between mouse and human thymocyte
378 development[61], differences in the systems used (iPSC-derived vs. thymus-derivates DP T cells)
379 or related to the transient expansion of a highly proliferative, immature intermediate ($CD4^-$ $CD8^+$
380 $Mki67^+$)[61]. Further characterization of the intermediate stages will shed light on the mechanisms
381 of positive selection induced by PMA/I in our system.

382 Initial characterization of iPSC-CD4sp T cells revealed interesting similarities and differences to
383 their primary T cell counterparts. The features observed in the iPSC-CD4sp cells may be due to
384 low levels of CD4 transcripts caused by the activated state of these cells compared to primary
385 CD4 T cells. Indeed, the cells maintained high levels of CD69 expression prior to activation when
386 compared to primary CD4 T cells (**Figure 5B**). Helper T cells often downregulate CD4 expression
387 upon chronic stimulation which may explain the reduced transcripts caused by exposure to PMAI/I
388 treatment[62]. Using CITEseq in combination with scRNAseq in the future will achieve a better
389 characterization of the iPSC-CD4sp identity than using scRNAseq alone[63].

390 The expression of *ZBTB16* (PLZF), the predominantly memory phenotype ($CD45RO^+CD62L^-$)
391 and secretion of IL-4 observed in the iPSC-CD4sp T cells may be due to thymocyte-thymocyte
392 (T-T) interactions that can generate $CD4^+$ T cells with similar characteristics through a pathway

393 originally described *in vitro*[64] and subsequently evidenced in MHC class II transactivator (CIITA)
394 transgenic mice[65] and human fetuses[66]. A study generating iPSC-CD8 T cells through an ATO
395 also showed high levels of *ZBTB16* and similarities to fetal type 1 innate-like T unconventional
396 cells, which are $CD8^+$, as classified by Cell Typist[13], suggesting that *in vitro* differentiation systems
397 such as ATOs that lack thymic epithelial cells (TECs) give rise to innate-like T cells resembling
398 fetal unconventional T cells. While the low levels of *CD4* transcripts did not allow a clear
399 classification of our iPSC-CD4sp T cells, their phenotype and transcriptional profile is evocative
400 of the innate and fetal unconventional T cells generated through T-T interactions[13]. Modification
401 of the differentiation process and integration of signals similar to those induced by TECs through
402 culture media optimization and/or cell engineering[67] might allow for the generation of CD4 T cells
403 with a more mature and less innate phenotype.

404 We did not detect IFN-γ from the iPSC-CD4sp T cells but observed secretion of pro-inflammatory
405 cytokines IL-2 and TNF-α upon stimulation, as well as Th2-like IL-10 and IL-4 cytokines[68 15]. This
406 profile is similar to fetal unconventional $CD4^+$ $PLZF^+$ T cells which, when stimulated, upregulate a
407 variety of cytokines not usually produced by a single Th subset[69]. Different levels of TCR activation
408 induce different cell fates and modifying the TCR activation levels might modify the cell fate
409 towards a Th1 vs. Th2 phenotype[70].

410 In addition to maintaining a serum- and feeder-free differentiation system, the use of PMA/I to
411 generate iPSC-CD4sp T cells is an especially critical finding as providing a positive selection
412 signal towards the CD4 lineage is the first step to generating Tregs. After maturation, the iPSC-
413 CD4sp T cells were treated with TGFβ, ATRA, IL-2 and a soluble CD3/CD28/CD2 activator to
414 convert them to a $FOXP3^+$ Treg phenotype. The generation of Tregs from naïve CD4 T cells using
415 TGFβ is well-documented[36]. While TGFβ-induced iTregs express FOXP3, they are only partially
416 demethylated at FOXP3 TSDR and are unstable in their expression of FOXP3. In addition,
417 polyclonal iTregs do not always display a regulatory phenotype, are not always suppressive and

418 can produce high levels of inflammatory cytokines[71]. In contrast, the iPSC-Tregs generated within
419 our system were highly demethylated at FOXP3 TSDR, suppressed Tconv proliferation and did
420 not produce inflammatory cytokines despite utilizing TGFβ towards its conversion. Transcriptomic
421 analysis by scRNA-seq further confirmed the identity and similarity of the iPSC Tregs to primary
422 Tregs as assessed by Cell Typist. The iPSC-Tregs expressed typical markers of their primary
423 natural Treg counterpart, namely highly expressing *FOXP3*, *IKZF2* and *IL2RA* in the absence of
424 activation. The iPSC-Tregs also expressed a previously published[12] core Treg signature[39-41]
425 similar to that of primary Tregs and less similar to iTregs and Tconv. Differential expression of
426 genes between iPSC-Treg and primary Treg, such as *IL7R* and *ID2*, could be due to culture
427 conditions or to differences between cells that differentiated *in vitro* as compared to *ex vivo* adult
428 cells. Finally, since scRNA-seq utilizes relative expression levels, measuring the absolute
429 expression of these markers by bulk RNA-seq may provide better quantitative results to
430 distinguish these populations.

431 Previous studies have shown that iPSCs derived from T cells express TCRαβ prematurely which
432 interferes with DP T cell formation and can be overcome by supplying the cells with a strong Notch
433 signal[11]. Constitutive expression of CAR with simultaneous expression of the endogenous TCR,
434 however, offsets the effects of a stronger Notch signal. In this case, both elimination of TRAC
435 expression as well as attenuation of the CAR signal was required to restore DP T cell generation[11,
436 12]. These are important considerations for the generation of a scalable cell therapy product using
437 engineered iPSCs. While we were able to generate DP T cells from both wild-type and engineered
438 iPSCs, the exact Notch ligand in the lymphocyte differentiation coating material (LDCM) reagent
439 is unknown making the need to test a known Notch ligand necessary for improving DP T cell
440 yields. In addition, we observed a lower yield of HLA-A2 CAR$^+$ iPSCs-Tregs as compared to Tregs
441 generated from unedited iPSCs, supporting the idea that premature TCR expression and CAR
442 signaling influences DP T cell yields and subsequent Treg generation. Defining the Notch ligand,

443 optimizing CAR signaling as well as applying compound-based measures to improve DP T cell
444 yield from iPSCs can aid in the generation of a more robust and reproducible differentiation
445 protocol [11].

446 Cryopreservation is key to the development and delivery of successful cell therapy products. We
447 found that our CAR iPSC-Tregs were amenable to cryopreservation and showed similar viability
448 pre- and post-cryopreservation with approximately 80% recovery post-thaw. The phenotype of the
449 cells was also maintained pre- and post-thaw with appreciable upregulation of CD69 post-
450 activation via the CAR or TCR. Importantly, the cryopreserved iPSC-Tregs suppress Tconv
451 proliferation in vitro confirming that the cells maintain functionality **(Figure 7)**.

452 In summary, we demonstrate here a method to generate functional and stable iPSC-derived Tregs
453 and CD4sp T cells that removes the inconsistencies and safety issues caused by using xenogenic
454 materials. iPSCs can serve as an endless supply of CD4sp T cells and Tregs with and without a
455 CAR for therapeutic applications and our study supports further development of this process for
456 clinical use in oncology and autoimmune diseases.

457 **Limitations of the study**

458 Further characterization of the iPSC-Tregs and iPSC-CD4sp T cells is still required, including
459 evaluation ability to expand to clinically relevant numbers and *in vivo* functions. Our initial
460 transcriptomics data shows that the iPSC-CD4sp T cells generated have an immature and
461 innate-like phenotype. Further optimization of the iPSC-CD4sp differentiation can be achieved
462 using a model-guided approach such as design of experiment (DOE) to optimize culture
463 conditions and a more in-depth multi-omics analysis to identify genes that can be modified
464 through genome engineering to obtain a more mature CD4 T cell phenotype. While we have
465 clearly shown that the iPSC-Tregs are functional *in vitro*, it is essential to test their suppressive
466 capacities and phenotypic stability *in vivo* in a GvHD mouse model.

467 ## Methods

468 **Generation of human induced pluripotent stem cell lines.** Previously cryopreserved CD4 T
469 cells were used for reprogramming to pluripotency. CD4 T cells were isolated from mobilized
470 leukapheresis material from a healthy male donor (AllCells, LLC) with informed written consent.
471 The raw material was washed several times to remove platelets, labeled with CD4 microbeads
472 (Miltenyi Biotec) and then isolated using the Miltenyi CliniMACS system. Isolated CD4 T cells
473 were analyzed for purity prior to cryopreservation. To prepare for reprogramming, the CD4 T cells
474 were thawed and cultured overnight in RPMI + 10% human AB serum (huABS, Valley Biomedical)
475 and activated 1:1 with CD3/CD28 Dynabeads in 100 U/mL of IL-2 (Thermofisher). The next day,
476 the CD4 T cells were debeaded and sorted for $CD4^{+}CD25^{+}$ cells and recovered overnight in RPMI
477 + 10% huABS with 100 U/mL of IL-2. One day post-sort, the sorted CD4 T cells were
478 reprogrammed with Sendai virus carrying the four transcription factors OCT, SOX2, KLF4, and C-
479 MYC as previously reported using Cytotune iPS-2.0 Sendai Reprogramming Kit (Thermofisher;
480 Fusaki Proc Japan Academy 2008). After transduction, cells were recovered in RPMI + 10%
481 huABS for 24 hours and transferred to ReproTeSR media (StemCell Technologies) on Matrigel-
482 coated plates (Corning). Cells were fed daily or every day until the appearance of colonies by day
483 14. Colonies were examined for appropriate morphology then manually selected for further
484 expansion and transition to mTeSR1 media (StemCell Technologies)

485 **Characterization of human induced pluripotent cells lines.** Immunocytochemical analysis for
486 pluripotency of iPSC lines was performed by washing cells in 1X PBS (Thermofisher), fixed in 4%
487 paraformaldehyde for 20 minutes at 4°C, and blocked in 10% normal goat or rabbit serum with
488 0.5% Triton X-100 (Sigma) in PBS. Immunocytochemical analysis was performed using primary
489 antibodies and corresponding AlexaFluor-conjugated secondary antibodies (Thermofisher). All
490 antibodies were diluted and used according to manufacturer's instructions. Cell nuclei were
491 counterstained with DAPI in some experiments[72]. Images were collected using an EVOS Cell

492 Imaging System (Thermofisher). PluriTest analysis was performed by ThermoFisher Scientific.
493 Karyotype analyses were performed by Cell Line Genetics.

494 **iPSC culture and clonal expansion.** iPSCs were maintained on Matrigel (Corning) in mTeSR1
495 media according to manufacturer's instructions (StemCell Technologies). For passaging, iPSC
496 colonies were detached briefly with either Accutase and manually scraped or with Gentle Cell
497 Dissociation Reagent. Cells were routinely passaged at a 1:8-1:10 split ratio in the presence of Y-
498 27632 (ROCK inhibitor, Tocris) for the first day after passaging and removed for subsequent media
499 changes.

500 For clonal expansion of transfected iPSCs, a method of low-density passaging was used. After
501 electroporation, iPSCs were passaged at a low seeding density (1e3, 2.5e3, 5e3 cells per well of
502 a 6-well plate) such that a single iPSC would give rise to a single colony in a Matrigel-coated 6-
503 well plate. iPSC colonies were then manually picked and expanded individually. Tightly packed
504 colonies with clearly defined borders were then collected for genomic DNA isolation and
505 subsequent screening for targeted integration.

506 **Differentiation of HSPCs from iPSCs**. iPSCs were differentiated as previously described with
507 modifications[24, 25]. Embryoid bodies were generated from iPSCs in APEL2 media (StemCell
508 Technologies) and cultured in non-tissue culture or ultra-low attachment 96-well round bottom
509 plates in the presence of 10 ng/mL BMP4, 10 ng/mL VEGF, 50 ng/mL SCF, 10 ng/mL bFGF, and
510 10 μM Y-27632 on day 0 (all cytokines from Thermofisher). EBs were then cultured in APEL2
511 media in the presence of 20 ng/mL VEGF, 10 ng/mL bFGF, 100 ng/mL SCF, 20 ng/mL FLT-3L, 20
512 ng/mL TPO and 40 ng/mL IL-3 from day 1 to day 6 with a media refresh every 2 days (all cytokines
513 from Thermofisher). On day 8, EBs were switched to complete StemPro-34 media (Thermofisher)
514 and supplemented with 100 ng/mL SCF, 20 ng/mL FLT3-L, 20 ng/mL TPO, and 40 ng/mL IL-3 in
515 order to expand developing HSPCs. Media was refreshed every 2 days until day 14. The EBs

516 were then collected and passed through a 70 μM cell strainer. The resulting cell suspension
517 containing the HSPCs was then used for downstream differentiation.

518 **Differentiation of T cell progenitors from iPSC-HSPCs.** StemDiff T cell kit (StemCell
519 Technologies) was used to differentiate HSPCs to lymphoid progenitor cells and to DP T cells.
520 Manufacturer's instructions were followed unless otherwise indicated. HSPCs were seeded at
521 50,000 cells/well of a 6-well plate coated with lymphocyte differentiation coating material (LDCM)
522 and cultured in StemSpan Lymphoid Progenitor Expansion Media to differentiate the HSPCs to
523 CD5+CD7+ lymphoid progenitor cells. After 14 days of culture (differentiation day 28), resulting
524 iPSC-lymphoid progenitor cells were harvested and seeded at 0.5e6/well of a 6-well plate with a
525 fresh coating of LDCM. The cells were cultured in StemSpan T Cell Progenitor Maturation Media
526 (maturation media) for differentiation to CD4+CD8+ DP T cells. After 14 days of culture
527 (differentiation day 42), the DP T cells were harvested for further differentiation.

528 **Generation of CD4-single positive T cells and Tregs from iPSC-DP T cells.** Induction of DP
529 T cells to CD4sp T cells was performed on LDCM in maturation media. On differentiation day 42,
530 a cell stimulation cocktail composed of phorbol 12-myristate 13-acetate and ionomycin was added
531 to the cultures at three different concentrations from the 500X stock concentration: low (0.01 μM
532 PMA, 0.16 μM Ionomycin), medium (0.02 PMA μM , 0.335 μM Ionomycin), and high (0.0405 μM
533 PMA, 0.67 μM Ionomycin). A full media change was performed 24 hours later by harvesting the
534 entire cell suspension, replating into fresh maturation media and seeding at a 1:1 ratio onto new
535 LDCM coated 6-well plates. The cells were then fed every 3-4 days for an additional week until
536 day 50. On day 50, the cells were then treated with 20 uL/mL of Immunocult Human Treg
537 Differentiation Supplement (StemCell Technologies) containing recombinant human TGF-B1 and
538 all-trans retinoic acid, 12.5 uL/mL of Immunocult Human CD3/CD28/CD2 T cell activator
539 (StemCell Technologies) and 10 ng/mL of CTS IL-2 (Thermofisher). Media in the wells for
540 conversion to Tregs was composed of a 50% mixture of complete CTS OpTmizer and maturation

541 media. A half media change was performed on day 54 with a 50% mixture of CTS OpTmizer and
542 maturation media supplemented with 10 ng/mL of IL-2.

543 **Flow cytometry, sorting and antibodies.** Flow cytometry was performed in FACS buffer
544 composed of PBS, 0.5% BSA, and 1 mM EDTA. For extracellular staining, antibodies were added
545 to cells according to manufacturer's instructions, incubated at 4°C for 20 minutes, and washed
546 before analysis. For intracellular staining, cells were first stained with extracellular markers and
547 fixed and permeabilized using the eBioscience FOXP3/Transcription Factor Staining Buffer set
548 (Thermofisher). Antibodies were then added according to manufacturer's instructions. Attune NxT
549 flow cytometer (Thermofisher) and Sony Sorter SH800 was used for flow cytometric analysis and
550 sorting, respectively. Antibodies (clones in parentheses) used for surface and intracellular staining
551 of the following molecules were obtained from Biolegend: CD45-FITC (Clone HI30, #304054),
552 FOXP3-AF647 (Clone 206D, #320114), ThPOK-PE (Clone 11H11A14, #656407), TCRab-PECy
553 (Clone IP26, #306720), Helios-PE (Clone 22F6, Cat# 137216), CD127-BV605 (Clone A019D5,
554 #351334), CD127-AF700 (Clone A019D5, #351344), CD28-FITC (Clone S20013F, #377612),
555 CD62L-PECy7 (Clone MEL-14, #104418), and PD-1-APC (Clone 12.2H7, #329908). Antibodies
556 against CD34-APC (Clone 581, #555824), CD25-PECy7 (Clone 2A3, #335789), CD45RO-BV421
557 (Clone UCHL1, #562641) and CD3-BV510 (Clone UCHT1, #563109) were obtained from BD
558 Biosciences. Antibodies against CD4-e450 (Clone OKT-4, #48-0047-42), CD4-PE (Clone OKT-4,
559 #12-0048-42), CD8-FITC (Clone SK1, #11-0087-42), and CD8-APC (Clone SK1, #11-0087-42)
560 were obtained from Thermofisher. CD69-APC (Clone REA824, #130-113-219), CD5-PE (Clone
561 UCHT1, #130-119-855) and CD7-APC (Clone CD7-687, #130-123-265) antibodies were obtained
562 from Miltenyi. An antibody to CD25-PE (Clone 2A3, #60153PE) was obtained from StemCell
563 Technologies. Antibodies to SOX2 (#MAB2018), OCT4 (#AF1759), SSEA-4 (#MAB1435) were
564 obtained from R&D Systems. TRA-1–81 (#MAB8495) was obtained from Santa Cruz
565 Biotechnology. The following fluorophore-conjugated secondary antibodies and DAPI were

566 obtained from Thermofisher: donkey-anti-mouse secondary antibody Alexa-Fluor 594 (#A21203)
567 and donkey-anti-goat secondary antibody Alexa-Fluor 488 (#A11055).

568 **scRNA-sequencing RNA extraction, library generation, and sequencing analysis.** RNA from
569 iPSC-Tregs, iPSC-CD4sp, primary Tregs, induced Tregs and primary Tconv was extracted using
570 an RNA extraction kit (Qiagen) following differentiation (iPSC-Tregs and induced Tregs) or
571 isolation and culture (primary Tregs and Tconv). Primary cells were isolated from leukapheresis.
572 Leukapheresis were obtained from healthy volunteers who provided written informed consent.

573 Single cell RNA-sequencing libraries were sequenced on a NextSeq 500. Samples had an
574 average depth of 18636 reads per cell. Read quality control, UMI counting, barcode counting, and
575 alignment to the GRCh38 GENCODE v32/Ensembl 98 reference genome from 10x Genomics
576 were performed using the "cellranger 6.0.2" pipeline. All downstream analysis were performed
577 using the Seurat packages in R for single-cell RNAseq analysis[73].

578 All samples were filtered on the following measures: number of unique genes detected, total
579 number of molecules detected, and level of expression of mitochondrial reads before integrating
580 the datasets. We removed cells in which greater than 20% mitochondrial reads, less than 200
581 feature counts, or greater than 6500 feature counts were detected.

582 The data was then normalized using the Seurat normalization function which divides the feature
583 counts by total counts for each cell, then multiplies the resulting fraction by a scale factor of
584 1.00e+4, and, lastly, log-normalizes this value.

585 Dimensionality reduction was performed using Seurat packages and utilizing principal
586 components 1 through 50 in the reduction. Clusters were determined at a resolution of 0.3. The
587 identity of each cluster was validated by evaluation of gene expression within each cluster of cell-
588 type specific markers for the cell-types of interest.

589 The Seurat object was exported and converted to an h5ad file to use CellTypist's automated cell
590 type annotation. CellTypist's Immune_All_High, Immune_All_Low, and Pan_Fetal_Human
591 models were used for the automated annotation of cell types[74]. The mode "prob match" was used
592 for the Pan_Fetal_Human model to assign multiple cell types per sample.

593 **Assessment of iPSC-CD4sp T cell and iPSC-Treg Function.** For assessment of Tconv or iPSC-
594 CD4sp T cell phenotype and activation, cells were sorted and cultured in X-VIVO15 (Lonza) +
595 10% huABS (Valley Biomedical). Cells were either left unactivated or activated with Immunocult
596 Human CD3/CD28/CD2 T cell activator per manufacturer's instructions (StemCell Technologies)
597 for 24 or 48hrs. Cells were then stained with indicated antibodies and run on flow cytometry as
598 previously described. For assessment of cytokine secretion, unactivated or activated iPSC-
599 CD4sp T cells were seeded at 5e4 cells/well in a round-bottom 96 well plate in 200 uL of media.
600 The supernatant was collected 24 hours later.

601 For assessment of iPSC-Treg function, cells were sorted on day 57 and cultured in complete
602 OpTmizer media supplemented with 1000U IL-2/mL (Thermofisher) for three days prior to
603 functional analysis. iPSC-Tregs were then activated with CD3/CD28 Dynabeads (Thermofisher)
604 at a ratio of 1:1 in media composed of X-VIVO15 (Lonza) + 10% huABS (Valley Biomedical) +
605 Penicillin / Streptomycin solution (pen/strep). For analysis of cytokine production, 5e4 activated
606 and unactivated cells were seeded in a round-bottom 96-well plate in 200 uL of media. One day
607 post-activation, supernatant was collected and analyzed for cytokines using human cytokine
608 assay X (Meso Scale Discovery). For assessment of Tconv suppression, activated and
609 unactivated iPSC-Tregs were co-cultured with activated (2:1 beads:cells) Tconv labeled with Cell
610 Trace Violet (Thermofisher) in X-VIVO15 media supplemented with pen/strep. iPSC-Tregs were
611 initially plated at 5e4/well in a 96-well round-bottom plate and serially diluted by a factor of 2 down
612 to 781.25 cells/well. 2.5e4 activated, CTV-labeled Tconv were then added to each serially diluted
613 well of iPSC-Tregs. Baseline Tconv proliferation was determined by culturing 2.5e4 Tconv in the

614 absence of iPSC-Tregs. Three days after co-culture, cells were collected, labeled for viability and
615 assessed for Tconv proliferation via Cell Trace Violet dye by flow cytometric analysis. For
616 assessment of iPSC-Treg cytolytic activity, activated and unactivated iPSC-Tregs were cocultured
617 with activated Tconv. 5e4 iPSC-Tregs were seeded with 5e4 primary Tconv and cultured for 3
618 days in X-VIVO15 media supplemented with pen/strep. The supernatant was then collected and
619 analyzed using the CyQuant LDH Cytotoxicity Kit (Thermofisher) following the manufacturer's
620 instructions. Samples were read on a SpectraMax microplate reader (Molecular Devices). Primary
621 Treg, Tconv and CD8 controls were cultured for 7-9 days prior to activation and assessment of
622 function.

623 **FOXP3 TSDR demethylation assay.** The Treg-specific demethylated region (TSDR)
624 hypomethylation status of FOXP3 gene was measured using a post-PCR High Resolution Melt
625 (HRM) analysis as previously described[6]. Briefly, genomic DNA was extracted from cell pellets
626 containing at least 1e6 cells/pellet using the DNeasy Blood and tissue kit (Qiagen), followed by
627 bisulfite conversion using the Epitech Fast Bisulfite Conversion Kit (Qiagen). The FOXP3 TSDR
628 regions were then amplified from the converted sample gDNAs by qPCR using specific primers
629 (forward: TTGGGTTAAGTTTGTTGTAGGATAG, reverse: ATCTAAACCCTATTATCACAACCCC,
630 Sigma Aldrich, USA) and Precision Melt Supermix (Biorad). The melting curves of amplified
631 product DNA fragments were quantified against the methylation standard curve generated using
632 commercial bisulfite converted human genomic DNAs (Qiagen) and expressed as a mean
633 methylation percentage.

634 **Cytokine MSD methods**. The concentrations of cytokines were measured with MSD U-Plex kits
635 (#K15067L-1, MSD, USA) following the manufacturer's protocol. Briefly, biotinylated capture
636 antibodies were incubated with specific linkers and then the mixture of linker coupled antibodies
637 was added to MSD U-Plex plates. After 1 hour incubation and wash step, standard curves and
638 samples were added to the plates. The plates were washed again after the sample incubation. A

639 mixture of SULFO-Tag conjugated detection antibodies was added to the wells and incubated.
640 After the final wash step, MSD GOLD Read Buffer B was added to the plate followed by reading
641 the electrochemiluminescence signals in a MESO SECTOR S 600 instrument.

642 **ZFN and donor DNA constructs**. The zinc finger nuclease (ZFN) pair targets the *TRAC* locus,
643 encoding for the alpha chain of the TCR, at exon 2. The ZFP backbone and FokI variants were
644 generated by reassembling zinc finger arrays from modules as previously described [75] and cloning
645 the resulting zinc finger array into a vector containing the desired FokI variant. All constructs were
646 verified by Sanger sequencing with two sequencing primers to yield overlapping sequence reads
647 of the entire ZFN coding sequence[76]. mRNA was transcribed from a PCR template using the 5×m
648 Message mMachine T7 ULTRA kit (Invitrogen) according to the manufacturer's instructions as
649 previously reported[76].

650 We designed and cloned the donor DNA sequence into a customized AAV vector containing AAV
651 inverted terminal repeats (ITRs). An AAV vector was initially selected to use AAV as DNA delivery
652 system but we ultimately optimized delivery using plasmid DNA. The pAAV-partial-TRAC-HLA-A2
653 CAR contains 110bp of genomic partial TRAC sequence (amplified by PCR) flanking the TRAC
654 homologous donor templates in frame with the second exon of TRAC, followed by a self-cleaving
655 T2A peptide, the HLA-A2 CAR and a bGHpA sequence.

656 **Transfection of TRAC-ZFN mRNA and donor DNA**. All transfections were performed on the
657 Maxcyte ATx (model GT) electroporation system. Approximately 3e6 iPSCs were used for
658 electroporation in an OC-100 processing assembly (Maxcyte). iPSCs were treated with Accutase
659 until cells were fully detached (~3min). After collection, cells were pelleted and washed once with
660 Maxcyte electroporation buffer. The iPSCs were then resuspended in Maxcyte electroporation
661 buffer at a concentration of 30e6 cells/mL and mixed with ZFN mRNA (10 ng/μl) and 8 ug of donor
662 DNA. The cell and nucleic acid mixture was dispensed into the OC-100 assembly and immediately
663 placed into the Maxcyte instrument using Optimization program 9. iPSCs were then recovered for

20 minutes at 37°C in the assembly and then transferred to Matrigel-coated plates in mTeSR1 media. Y-27632 was added to the media for 2-3 days post-transduction until confluent and then passaged for clonal expansion.

Analysis of targeted integration in iPSCs. iPSCs were assessed quantitatively for on-target insertions/deletions and targeted integration through NGS sequencing on the Illumina platform. Genomic DNA from clonally expanded iPSCs was first amplified, followed by nested PCR amplification to prepare ~200 bp amplicons for paired-end deep sequencing on the Illumina MiSeq sequencer.

iPSC-Treg Cryopreservation. Post-sort CAR iPSC-Tregs were recovered in complete OpTmizer supplemented with 1000U IL-2/mL at a concentration of 1e6/mL. 24 hours after recovery, CAR iPS-Tregs were harvested, counted and cryopreserved in CryoStor CS10 (Biolife Solutions) at a concentration of 4-5e6/mL. Cryopreserved cells were placed in an alcohol-free freezing container (CoolCell, Corning) and placed at -80C overnight before transferring to LN2 for long-term storage.

Data Availability. Data will be made available upon reasonable request. Sequencing data to prove targeted insertion and scRNAseq data will be deposited on relevant NCBI archives before publication and access codes will be shared. Due to the proprietary nature of the donor plasmid sequence we have restricted data access to the full-length sequencing data of the insert for the edited iPSC cell lines as described in the manuscript.

Material Availability. For this research we have derived unique iPSC lines (edited and non-edited) from human T cells and developed proprietary Zinc finger nucleases (ZFN). We are restricting access to these lines and ZFN sequences and mRNA to protect Sangamo Therapeutics' proprietary work. Any other requested materials will be reviewed on a case-by-case base and be subject to a Material Transfer Agreement.

Ethics Statement. The leukapheresis collection at AllCells, LLC used for the derivation of the iPSC cell line was approved by an independent review board (Alpha IRB) under the study title "Non-Mobilized Mononuclear Cell Apheresis Collection from Healthy Donors for the Research Market" (Protocol number: 7000-SOP-045). Informed consent was obtained from the cell donor. Specially trained nurses at LeukoLab, a division of AllCells, collected the leukopack from the donor. The donor was compensated for their time and effort related to their participation in the study as approved by the IRB.

695 **References**

696 1. Themeli, M., Riviere, I. & Sadelain, M. New cell sources for T cell engineering and
697 adoptive immunotherapy. *Cell Stem Cell* **16**, 357-366 (2015).
698 2. Hu, X. et al. Hypoimmune anti-CD19 chimeric antigen receptor T cells provide lasting
699 tumor control in fully immunocompetent allogeneic humanized mice. *Nat Commun* **14**,
700 2020 (2023).
701 3. Hu, X. et al. Hypoimmune induced pluripotent stem cells survive long term in fully
702 immunocompetent, allogeneic rhesus macaques. *Nat Biotechnol* **42**, 413-423 (2023).
703 4. Dominguez-Villar, M. & Hafler, D.A. Regulatory T cells in autoimmune disease. *Nat*
704 *Immunol* **19**, 665-673 (2018).
705 5. Sanders, J.M., Jeyamogan, S., Mathew, J.M. & Leventhal, J.R. Foxp3+ regulatory T cell
706 therapy for tolerance in autoimmunity and solid organ transplantation. *Front Immunol*
707 **13**, 1055466 (2022).
708 6. Proics, E. et al. Preclinical assessment of antigen-specific chimeric antigen receptor
709 regulatory T cells for use in solid organ transplantation. *Gene Ther* **30**, 309-322 (2023).
710 7. Raffin, C., Vo, L.T. & Bluestone, J.A. T(reg) cell-based therapies: challenges and
711 perspectives. *Nat Rev Immunol* **20**, 158-172 (2020).
712 8. Themeli, M. et al. Generation of tumor-targeted human T lymphocytes from induced
713 pluripotent stem cells for cancer therapy. *Nat Biotechnol* **31**, 928-933 (2013).
714 9. Nishimura, T. et al. Generation of rejuvenated antigen-specific T cells by reprogramming
715 to pluripotency and redifferentiation. *Cell Stem Cell* **12**, 114-126 (2013).

716 10. Montel-Hagen, A. et al. Organoid-Induced Differentiation of Conventional T Cells from
717 Human Pluripotent Stem Cells. *Cell Stem Cell* **24**, 376-389 e378 (2019).
718 11. van der Stegen, S.J.C. et al. Generation of T-cell-receptor-negative CD8ab-positive CAR T
719 cells from T-cell-derived induced pluripotent stem cells. *Nature biomedical engineering*
720 **6**, 1284-1297 (2022).
721 12. Li, S. et al. Strength of CAR signaling determines T cell versus ILC differentiation from
722 pluripotent stem cells. *Cell Rep* **42**, 112241 (2023).
723 13. Suo, C. et al. Mapping the developing human immune system across organs. *Science* **376**,
724 eabo0510 (2022).
725 14. Wang, Z. et al. 3D-organoid culture supports differentiation of human CAR(+) iPSCs into
726 highly functional CAR T cells. *Cell Stem Cell* **29**, 515-527 e518 (2022).
727 15. Yano, H. et al. Guided Polarization of iPSC-Derived CD4SP Helper T Cells By CRISPR/Cas9-
728 Based Genome-Editing. *Blood* **134**, 1937-1937 (2019).
729 16. Borst, J., Ahrends, T., Babala, N., Melief, C.J.M. & Kastenmüller, K. CD4+ T cell help in
730 cancer immunology and immunotherapy. *Nature Reviews Immunology* **18**, 635-647
731 (2018).
732 17. Turtle, C.J. et al. CD19 CAR-T cells of defined CD4+:CD8+ composition in adult B cell ALL
733 patients. *J Clin Invest* **126**, 2123-2138 (2016).
734 18. Sommermeyer, D. et al. Chimeric antigen receptor-modified T cells derived from defined
735 CD8+ and CD4+ subsets confer superior antitumor reactivity in vivo. *Leukemia* **30**, 492-
736 500 (2016).

737 19. Melenhorst, J.J. et al. Decade-long leukaemia remissions with persistence of CD4+ CAR T
738 cells. *Nature* **602**, 503-509 (2022).
739 20. Tay, R.E., Richardson, E.K. & Toh, H.C. Revisiting the role of CD4(+) T cells in cancer
740 immunotherapy-new insights into old paradigms. *Cancer Gene Ther* **28**, 5-17 (2021).
741 21. Vizcardo, R. et al. Regeneration of human tumor antigen-specific T cells from iPSCs
742 derived from mature CD8(+) T cells. *Cell Stem Cell* **12**, 31-36 (2013).
743 22. Iriguchi, S. et al. A clinically applicable and scalable method to regenerate T-cells from
744 iPSCs for off-the-shelf T-cell immunotherapy. *Nature communications* **12**, 430 (2021).
745 23. Chang, C.W., Lai, Y.S., Lamb, L.S., Jr. & Townes, T.M. Broad T-cell receptor repertoire in T-
746 lymphocytes derived from human induced pluripotent stem cells. *PLoS One* **9**, e97335
747 (2014).
748 24. Ng, E.S., Davis, R., Stanley, E.G. & Elefanty, A.G. A protocol describing the use of a
749 recombinant protein-based, animal product-free medium (APEL) for human embryonic
750 stem cell differentiation as spin embryoid bodies. *Nat Protoc* **3**, 768-776 (2008).
751 25. Kotini, A.G. et al. Stage-Specific Human Induced Pluripotent Stem Cells Map the
752 Progression of Myeloid Transformation to Transplantable Leukemia. *Cell Stem Cell* **20**,
753 315-328 e317 (2017).
754 26. Schmitt, T.M., Ciofani, M., Petrie, H.T. & Zuniga-Pflucker, J.C. Maintenance of T cell
755 specification and differentiation requires recurrent notch receptor-ligand interactions. *J*
756 *Exp Med* **200**, 469-479 (2004).
757 27. Trotman-Grant, A.C. et al. DL4-mubeads induce T cell lineage differentiation from stem
758 cells in a stromal cell-free system. *Nat Commun* **12**, 5023 (2021).

759 28. Mohtashami, M., Brauer, P.M. & Zuniga-Pflucker, J.C. Induction of Human T Cell
760 Development In Vitro with OP9-DL4-7FS Cells Expressing Human Cytokines. *Methods*
761 *Mol Biol* **2580**, 249-260 (2023).
762 29. Singer, A., Adoro, S. & Park, J.H. Lineage fate and intense debate: myths, models and
763 mechanisms of CD4- versus CD8-lineage choice. *Nat Rev Immunol* **8**, 788-801 (2008).
764 30. Jameson, S.C., Hogquist, K.A. & Bevan, M.J. Positive selection of thymocytes. *Annu Rev*
765 *Immunol* **13**, 93-126 (1995).
766 31. Ohoka, Y. et al. In vitro differentiation and commitment of CD4+ CD8+ thymocytes to the
767 CD4 lineage, without TCR engagement. *Int Immunol* **8**, 297-306 (1996).
768 32. Takahama, Y., Suzuki, H., Katz, K.S., Grusby, M.J. & Singer, A. Positive selection of CD4+ T
769 cells by TCR ligation without aggregation even in the absence of MHC. *Nature* **371**, 67-70
770 (1994).
771 33. Park, J.H. et al. Signaling by intrathymic cytokines, not T cell antigen receptors, specifies
772 CD8 lineage choice and promotes the differentiation of cytotoxic-lineage T cells. *Nat*
773 *Immunol* **11**, 257-264 (2010).
774 34. Fu, S. et al. TGF-beta induces Foxp3 + T-regulatory cells from CD4 + CD25 - precursors.
775 *Am J Transplant* **4**, 1614-1627 (2004).
776 35. Chen, W. et al. Conversion of peripheral CD4+CD25- naive T cells to CD4+CD25+
777 regulatory T cells by TGF-beta induction of transcription factor Foxp3. *J Exp Med* **198**,
778 1875-1886 (2003).

779 36. Mitsuhiro, K., Hiroko, N., Masahiro, O., Qianjin, L. & Akihiko, Y. Induced Regulatory T
780 Cells: Their Development, Stability, and Applications. *Trends in Immunology* **37**, 803-811
781 (2016).
782 37. Dominguez Conde, C. et al. Cross-tissue immune cell analysis reveals tissue-specific
783 features in humans. *Science* **376**, eabl5197 (2022).
784 38. Xu, C. et al. Automatic cell-type harmonization and integration across Human Cell Atlas
785 datasets. *Cell* **186**, 5876-5891 e5820 (2023).
786 39. Pesenacker, A.M. et al. Treg gene signatures predict and measure type 1 diabetes
787 trajectory. *JCI Insight* **4**, e123879 (2019).
788 40. Pesenacker, A.M. et al. A Regulatory T-Cell Gene Signature Is a Specific and Sensitive
789 Biomarker to Identify Children With New-Onset Type 1 Diabetes. *Diabetes* **65**, 1031-1039
790 (2016).
791 41. Höllbacher, B. et al. Transcriptomic Profiling of Human Effector and Regulatory T Cell
792 Subsets Identifies Predictive Population Signatures. *ImmunoHorizons* **4**, 585-596 (2020).
793 42. Huehn, J., Polansky, J.K. & Hamann, A. Epigenetic control of FOXP3 expression: the key to
794 a stable regulatory T-cell lineage? *Nat Rev Immunol* **9**, 83-89 (2009).
795 43. Floess, S. et al. Epigenetic control of the foxp3 locus in regulatory T cells. *PLoS Biol* **5**, e38
796 (2007).
797 44. Dikiy, S. & Rudensky, A.Y. Principles of regulatory T cell function. *Immunity* **56**, 240-255
798 (2023).
799 45. Vignali, D.A., Collison, L.W. & Workman, C.J. How regulatory T cells work. *Nat Rev*
800 *Immunol* **8**, 523-532 (2008).

801 46. Moore, K.W., de Waal Malefyt, R., Coffman, R.L. & O'Garra, A. Interleukin-10 and the
802 interleukin-10 receptor. *Annu Rev Immunol* **19**, 683-765 (2001).
803 47. Louey, A., Hernandez, D., Pebay, A. & Daniszewski, M. Automation of Organoid Cultures:
804 Current Protocols and Applications. *SLAS Discov* **26**, 1138-1147 (2021).
805 48. Seki, T. et al. Generation of induced pluripotent stem cells from human terminally
806 differentiated circulating T cells. *Cell Stem Cell* **7**, 11-14 (2010).
807 49. Loh, Y.H. et al. Reprogramming of T cells from human peripheral blood. *Cell Stem Cell* **7**,
808 15-19 (2010).
809 50. Brown, M.E. et al. Derivation of induced pluripotent stem cells from human peripheral
810 blood T lymphocytes. *PLoS One* **5**, e11373 (2010).
811 51. Hernandez, J.B., Newton, R.H. & Walsh, C.M. Life and death in the thymus--cell death
812 signaling during T cell development. *Curr Opin Cell Biol* **22**, 865-871 (2010).
813 52. Nagano, S. et al. High Frequency Production of T Cell-Derived iPSC Clones Capable of
814 Generating Potent Cytotoxic T Cells. *Mol Ther Methods Clin Dev* **16**, 126-135 (2020).
815 53. Kawamoto, H., Masuda, K. & Nagano, S. Regeneration of antigen-specific T cells by using
816 induced pluripotent stem cell (iPSC) technology. *Int Immunol* **33**, 827-833 (2021).
817 54. Maeda, T. et al. Regeneration of Tumor-Antigen-Specific Cytotoxic T Lymphocytes from
818 iPSCs Transduced with Exogenous TCR Genes. *Mol Ther Methods Clin Dev* **19**, 250-260
819 (2020).
820 55. Awong, G. et al. Human proT-cells generated in vitro facilitate hematopoietic stem cell-
821 derived T-lymphopoiesis in vivo and restore thymic architecture. *Blood* **122**, 4210-4219
822 (2013).

823 56. Edgar, J.M., Michaels, Y.S. & Zandstra, P.W. Multi-objective optimization reveals time- and
824 dose-dependent inflammatory cytokine-mediated regulation of human stem cell derived
825 T-cell development. *NPJ Regen Med* **7**, 11 (2022).
826 57. Klein, L., Robey, E.A. & Hsieh, C.S. Central CD4(+) T cell tolerance: deletion versus
827 regulatory T cell differentiation. *Nat Rev Immunol* **19**, 7-18 (2019).
828 58. Ashby, K.M. & Hogquist, K.A. A guide to thymic selection of T cells. *Nat Rev Immunol* **24**,
829 103-117 (2024).
830 59. Takahama, Y. & Nakauchi, H. Phorbol ester and calcium ionophore can replace TCR
831 signals that induce positive selection of CD4 T cells. *The Journal of Immunology* **157**,
832 1508-1513 (1996).
833 60. Karimi, M.M. et al. The order and logic of CD4 versus CD8 lineage choice and
834 differentiation in mouse thymus. *Nat Commun* **12**, 99 (2021).
835 61. Li, Y. et al. Development of double-positive thymocytes at single-cell resolution. *Genome*
836 *Med* **13**, 49 (2021).
837 62. Grishkan, I.V., Ntranos, A., Calabresi, P.A. & Gocke, A.R. Helper T cells down-regulate CD4
838 expression upon chronic stimulation giving rise to double-negative T cells. *Cell Immunol*
839 **284**, 68-74 (2013).
840 63. Stoeckius, M. et al. Simultaneous epitope and transcriptome measurement in single
841 cells. *Nat Methods* **14**, 865-868 (2017).
842 64. Park, S.H. et al. HLA-DR expression in human fetal thymocytes. *Hum Immunol* **33**, 294-
843 298 (1992).

844 65. Choi, E.Y. et al. Thymocyte-thymocyte interaction for efficient positive selection and
845 maturation of CD4 T cells. *Immunity* **23**, 387-396 (2005).
846 66. Lee, Y.J. et al. Generation of PLZF+ CD4+ T cells via MHC class II-dependent thymocyte-
847 thymocyte interaction is a physiological process in humans. *J Exp Med* **207**, 237-246
848 (2010).
849 67. Jing, R. et al. EZH1 repression generates mature iPSC-derived CAR T cells with enhanced
850 antitumor activity. *Cell Stem Cell* **29**, 1181-1196.e1186 (2022).
851 68. Butcher, M.J. & Zhu, J. Recent advances in understanding the Th1/Th2 effector choice.
852 *Fac Rev* **10**, 30 (2021).
853 69. Locher, V. et al. Homeostatic cytokines reciprocally modulate the emergence of prenatal
854 effector PLZF+CD4+ T cells in humans. *JCI Insight* **8**, e164672 (2023).
855 70. Hwang, J.R., Byeon, Y., Kim, D. & Park, S.G. Recent insights of T cell receptor-mediated
856 signaling pathways for T cell activation and development. *Exp Mol Med* **52**, 750-761
857 (2020).
858 71. Tran, D.Q., Ramsey, H. & Shevach, E.M. Induction of FOXP3 expression in naive human
859 CD4+FOXP3 T cells by T-cell receptor stimulation is transforming growth factor-beta
860 dependent but does not confer a regulatory phenotype. *Blood* **110**, 2983-2990 (2007).
861 72. Fong, H. et al. Genetic correction of tauopathy phenotypes in neurons derived from
862 human induced pluripotent stem cells. *Stem Cell Reports* **1**, 226-234 (2013).
863 73. Hao, Y. et al. Dictionary learning for integrative, multimodal and scalable single-cell
864 analysis. *Nat Biotechnol* **42**, 293-304 (2024).

865 74. Xu, C. et al. Automatic cell-type harmonization and integration across Human Cell Atlas
866 datasets. *Cell* **186**, 5876-5891 e5820 (2023).
867 75. Paschon, D.E. et al. Diversifying the structure of zinc finger nucleases for high-precision
868 genome editing. *Nat Commun* **10**, 1133 (2019).
869 76. Miller, J.C. et al. Enhancing gene editing specificity by attenuating DNA cleavage kinetics.
870 *Nat Biotechnol* **37**, 945-952 (2019).
871
872

Acknowledgements. We thank Prof. Maria Themeli for critical review of the manuscript and for giving critical advice for our research work. We also thank Prof. Megan Levings for critical advice on the transcriptomics analysis; Dr. Andreas Reik, Dr. Lei Zhang, Dr. George Kwong and Dr. Steven Cincotta for technical assistance; Dr. Julie Gertner-Dardenne, Dr. Maurus de la Rosa, Dr. David Fenard, Dr. Tobias Abel and Dr. Virginie Fabre for scientific discussions; Cayla McEwen and Jean Alladin for administrative support.

Patents. Part of this research work is described in the following patents:

US Patent number 11512287: “Targeted disruption of T cell and/or HLA receptors”

Application PCT/US2021/057152 (Filed Oct 28, 2021): “Generation of CD4+ Effector and Regulatory T cells from Human Pluripotent Stem Cells”

Application PCT/US2020/059730 (Filed Sep 11, 2020): “Generation of Engineered Regulatory T cells”

Author contributions. H.F., M.M., L.N., G.L., S.G., A.C. and S.Z. conception and design; H.F., M.M., J.J., L.N., K.K., S.S., J.H. and A.V. collection and/or assembly of data; H.F., M.M., J.J., L.N., K.K., G.L., S.G., S.S., J.H. and A.V. data analysis; H.F., M.M., L.N., S.S., A.C., J.F. and S.Z. data interpretation; J.F. advice on experimental design; A.C. and S.Z. study supervision; H.F. and S.Z. manuscript writing.

Competing interests. All authors are current or former Sangamo Therapeutics employees and shareholders.

Correspondence and requests for materials should be addressed to M.M., H.F. and S.Z.

MAIN FIGURES

FIGURE 1. Differentiation of iPSCs to HSPCs, lymphoid progenitors and DP T cells in serum- and feeder-free conditions.

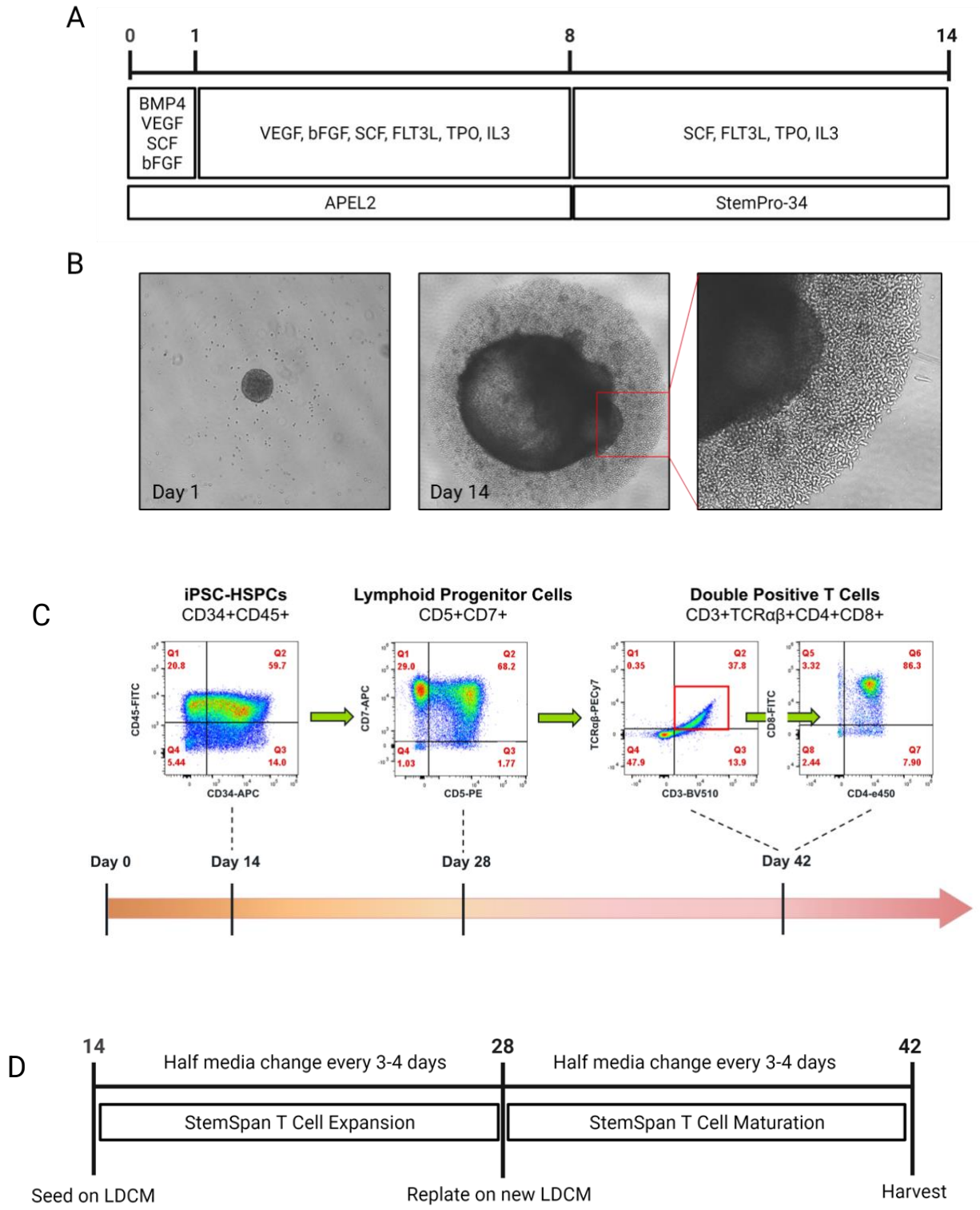

Figure 1. Differentiation of iPSCs to hematopoietic stem and progenitor cells (HSPCs), lymphoid progenitors and double positive (DP) T cells in serum- and feeder-free conditions.

A. Schematic for differentiation of iPSCs to HPSCs.
B. Embryoid bodies (EBs) at day 1 and 14 of differentiation. HSPCs emerged from the EB by day 14 and appeared as loosely packed cells (inset).
C. Representative flow cytometric analyses of HSPCs, lymphoid progenitor cells, and DP T cells from iPSCs. Cells were analyzed for phenotype over a 42-day period at the indicated timepoints. Data show one representative flow plot set of n=3 independent experiments from n=3 clones.
D. Schematic for differentiation of iPSC-HSPCs to lymphoid progenitor cells and DP T cells.

FIGURE 2. Cell Yield per Input iPSC.

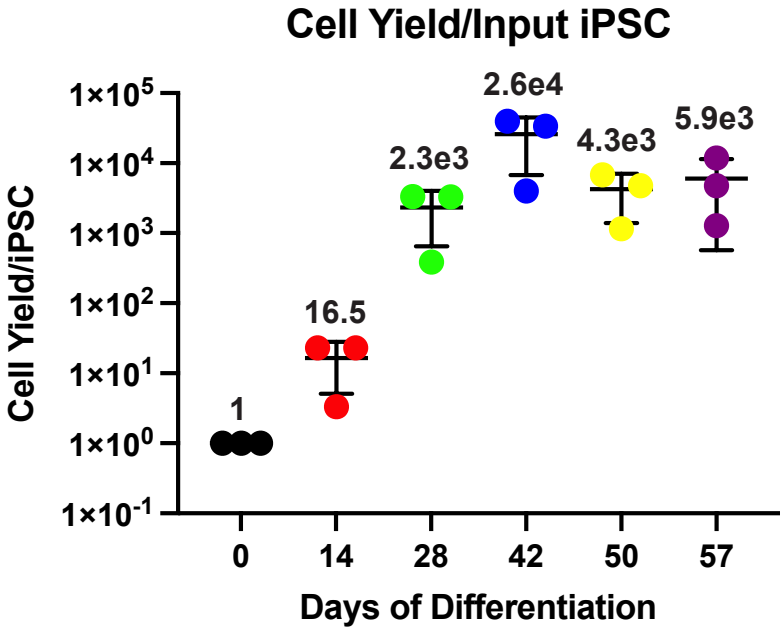

Figure 2. Yield of iPSC-derived hematopoietic stem and progenitor cells (HSPCs), lymphoid progenitors, double positive (DP) T cells, CD4sp T cells, and Tregs. Cell yield per input iPSC at various stages of differentiation. Data represent mean ± SD of n=3 independent experiments from n=1 clone.

FIGURE 3. Differentiation of iPSCs to CD4sp T cells and Tregs in serum- and feeder-free conditions.

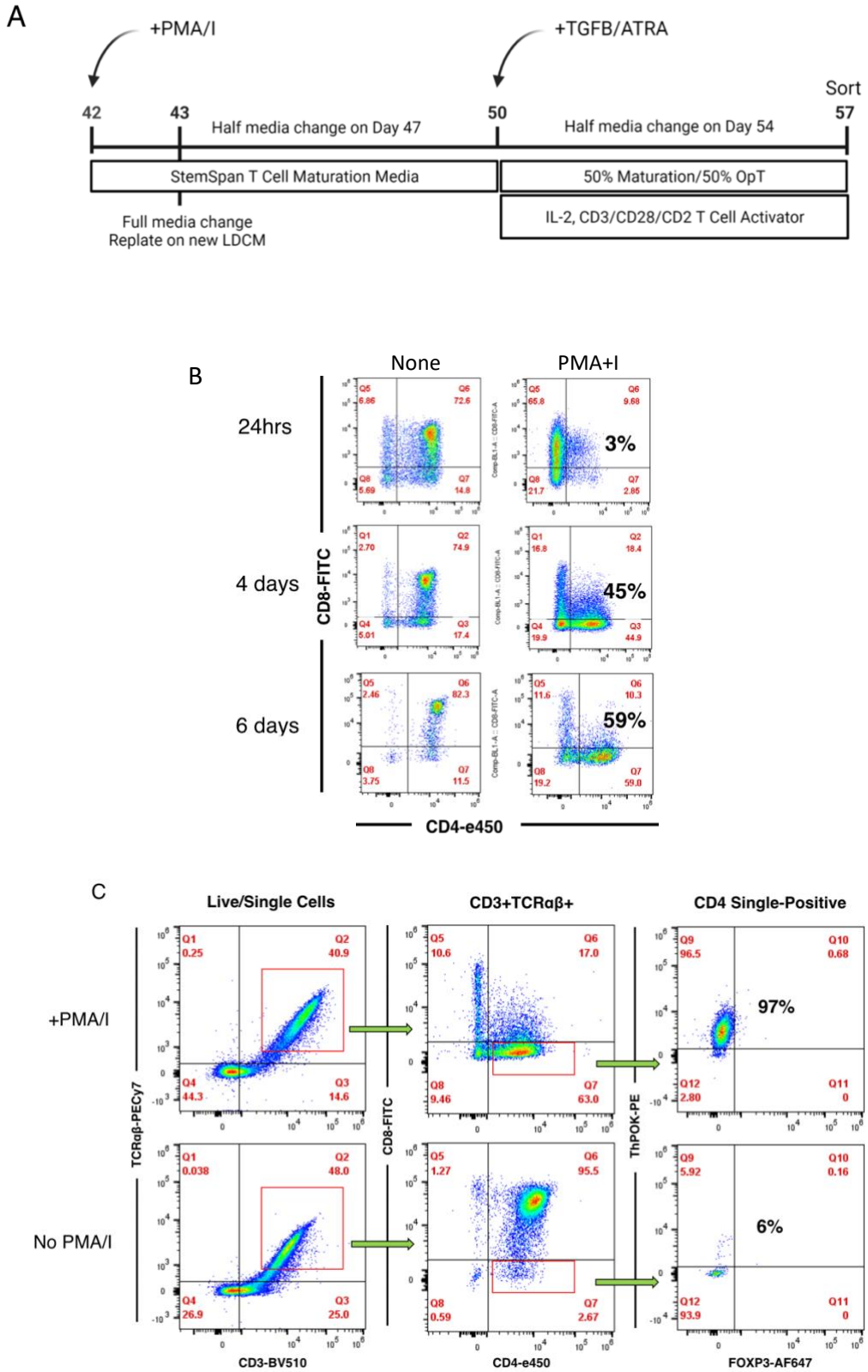

D

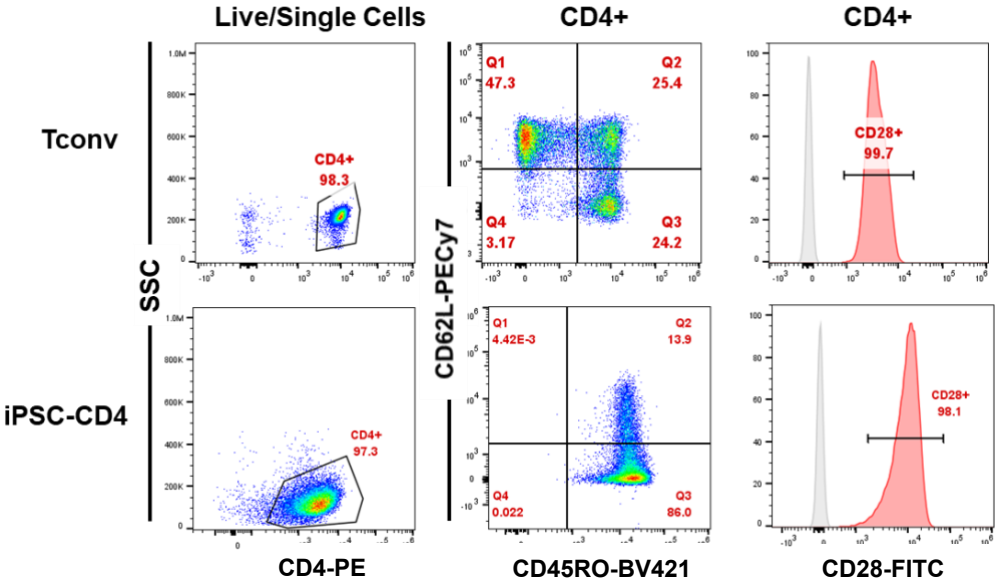
Live/Single Cells
CD4+
CD4+
Tconv
iPSC-CD4
SSC
CD4+
98.3
CD4+
97.3
CD62L-PECy7
Q1
47.3
Q2
25.4
Q4
3.17
Q3
24.2
Q1
4.42E-3
Q2
13.9
Q4
0.022
Q3
86.0
CD28+
99.7
CD28+
98.1
CD4-PE
CD45RO-BV421
CD28-FITC

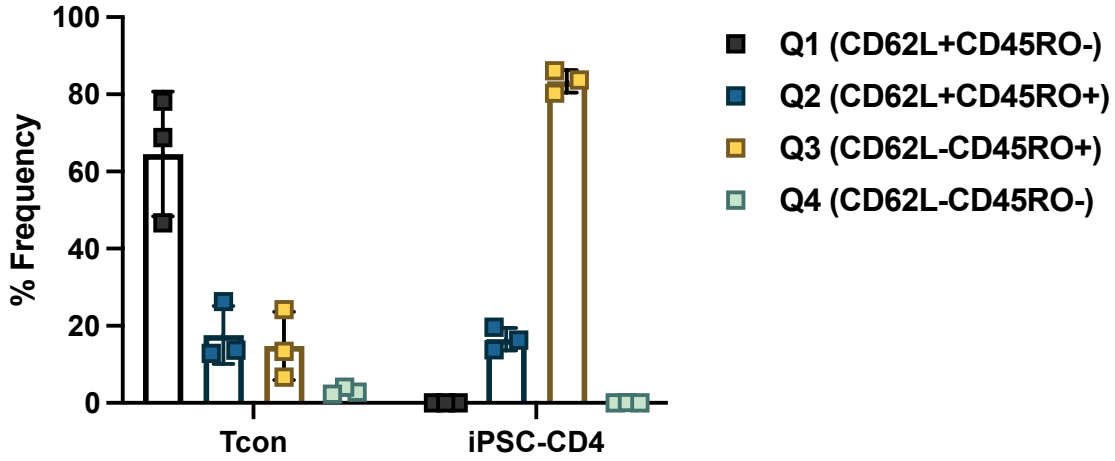
% Frequency
100
80
60
40
20
0
Tcon
iPSC-CD4
Q1 (CD62L+CD45RO-)
Q2 (CD62L+CD45RO+)
Q3 (CD62L-CD45RO+)
Q4 (CD62L-CD45RO-)

E

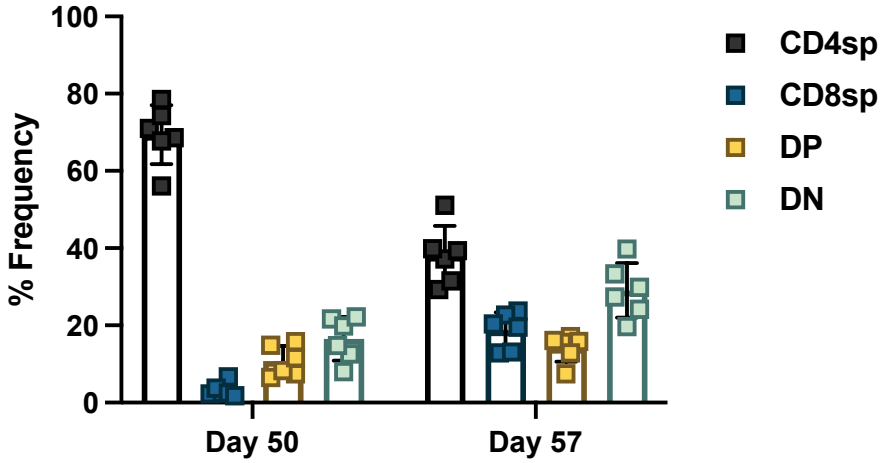
100
80
60
40
20
0
% Frequency
Day 50
Day 57
CD4sp
CD8sp
DP
DN

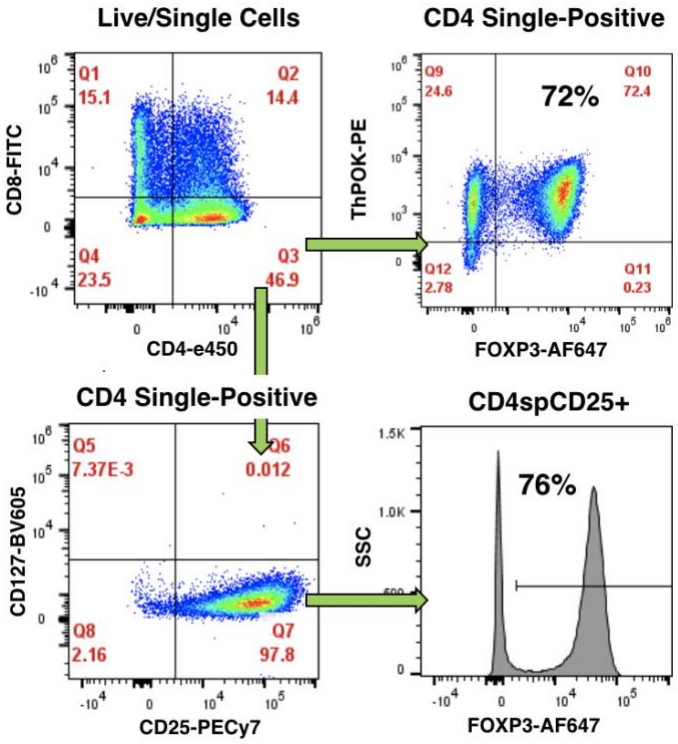
Live/Single Cells
Q1
15.1
Q2
14.4
Q4
23.5
Q3
46.9
CD8-FITC
CD4-e450
CD4 Single-Positive
Q9
24.6
Q10
72.4
72%
Q12
2.78
Q11
0.23
ThPOK-PE
FOXP3-AF647
CD4 Single-Positive
Q5
7.37E-3
Q6
0.012
Q8
2.16
Q7
97.8
CD127-BV605
CD25-PECy7
CD4spCD25+
76%
SSC
FOXP3-AF647

Figure 3. Differentiation of iPSCs to CD4sp T cells and Tregs in serum- and feeder-free conditions.

A. Schematic for differentiation of iPSCs to CD4sp T cells and Tregs.
B. Representative kinetic analysis of developing CD4sp T cells after Phorbol 12-myristate 13-acetate and Ionomycin (PMA/I) addition (low dose). Phenotype was assessed by the expression levels of CD4 and CD8 by flow cytometry (n=10 experiments from n=3 clones).
C. Representative flow plots of iPSC-CD4sp T cells 8 days after PMA/I addition (day 50 of differentiation) to assess for CD4 commitment. Phenotype was assessed by the expression levels of CD3, TCRαβ, CD4, CD8, FOXP3 and ThPOK in cells with and without PMA/I treatment (n=6 experiments from n=3 clones).
D. Representative flow plots and expression of CD4 markers in unactivated T conventional (Tconv)–and sorted unactivated iPSC-CD4sp T cells. Phenotype was assessed by flow cytometric analysis (n=3 experiments from n=1 clone) in Tconv and iPSC-CD4sp at day 50 of differentiation for the expression of CD4, CD62L, CD45RO and CD28. CD28 FMO control (gray) and CD28 expression (red).
E. Frequency of cell subpopulations from all live cells at day 50 and day 57 of differentiation (top) and representative flow cytometric plots of iPSC-Tregs 7 days after TGFβ+ATRA addition (day 57 of differentiation) (bottom). CD4sp, CD8sp, double positive (DP), and double negative (DN) populations were assessed by flow cytometric analysis of CD4 and CD8 expression (n=6 experiments from n=3 clones).

Data show either a representative flow plot set of n independent experiments or represent mean ± SD of n independent experiments.

FIGURE 4. Single cell gene expression analysis of iPSC-CD4sp and iPSC-Tregs.

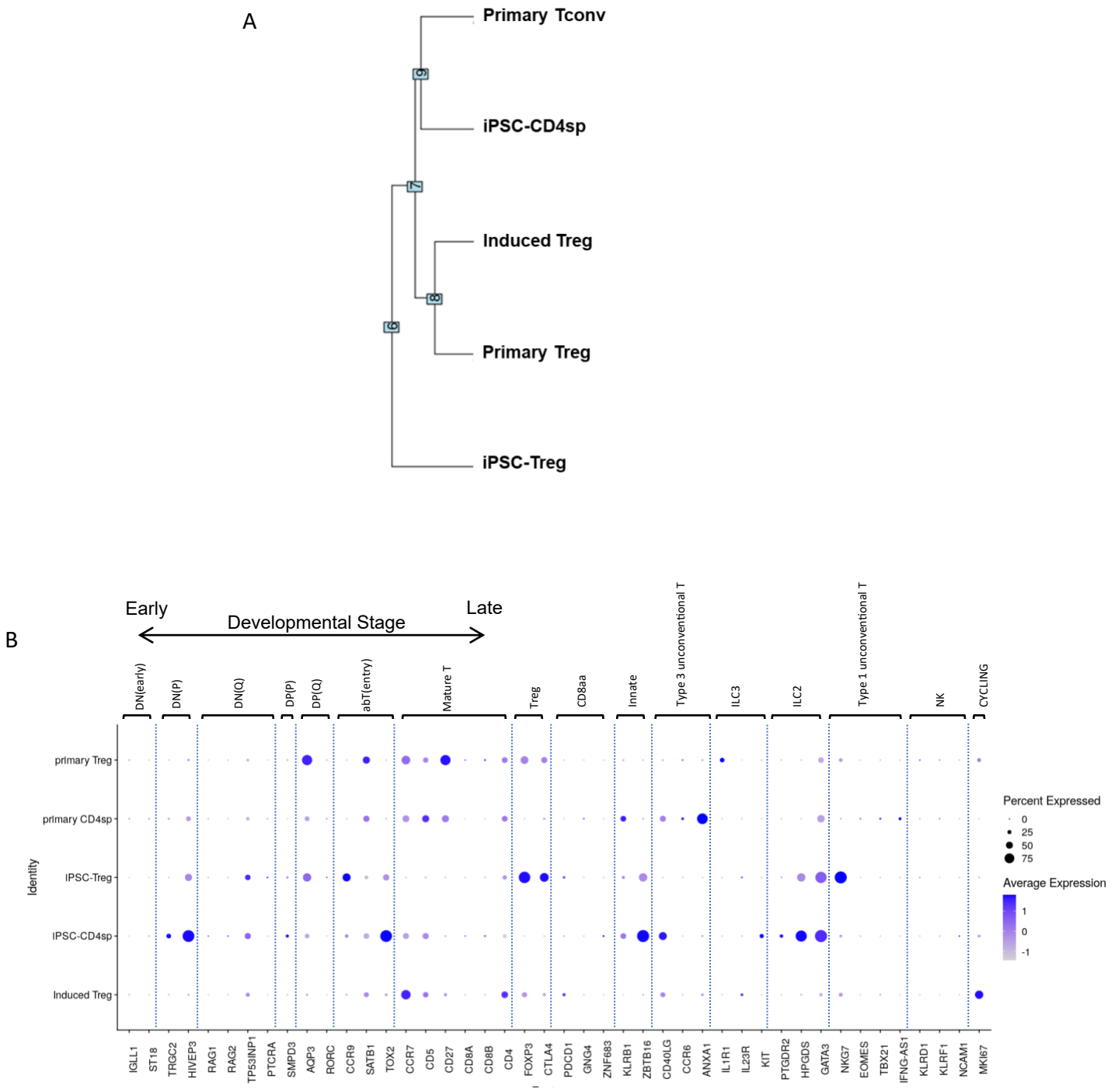

C

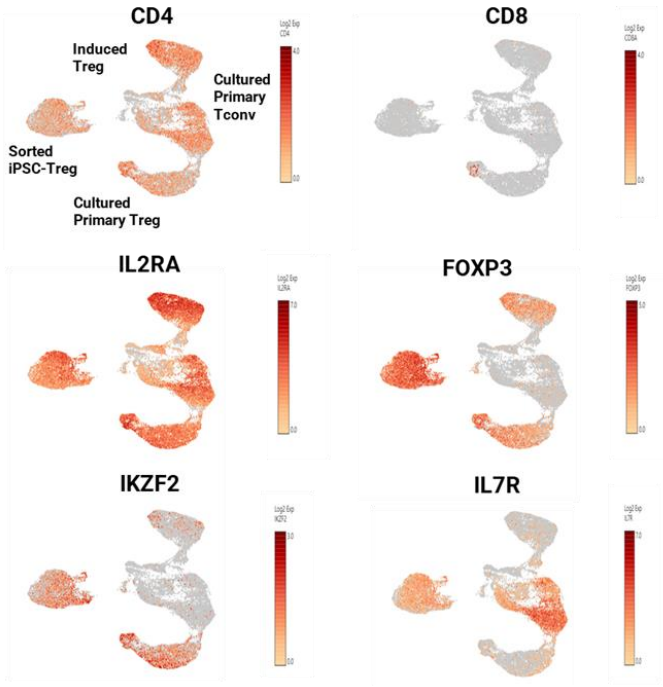
CD4
Induced Treg
Cultured Primary Tconv
Sorted iPSC-Treg
Cultured Primary Treg
CD8
IL2RA
FOXP3
IKZF2
IL7R

D

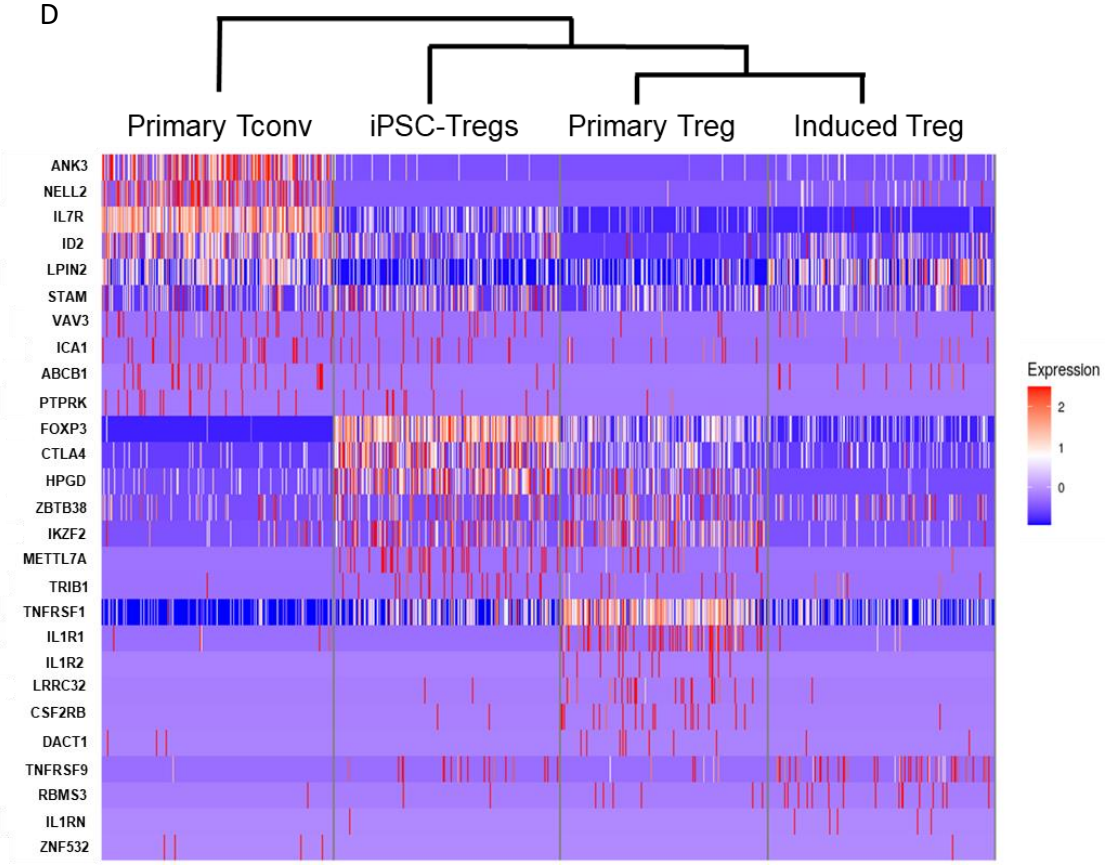
Primary Tconv
iPSC-Tregs
Primary Treg
Induced Treg
ANK3
NELL2
IL7R
ID2
LPIN2
STAM
VAV3
ICA1
ABCB1
PTPRK
FOXP3
CTLA4
HPGD
ZBTB38
IKZF2
METTL7A
TRIB1
TNFRSF1
IL1R1
IL1R2
LRRC32
CSF2RB
DACT1
TNFRSF9
RBMS3
IL1RN
ZNF532
Expression
2
1
0

Figure 4. Single cell gene expression analysis of iPSC-CD4sp and iPSC-Tregs.

A. Hierarchical clustering of iPSC-Tregs, iPSC-CD4sp Tcells, cultured primary T conventional (Tconv), cultured primary Treg and induced Tregs based on differentially expressed genes (DEGs). DEGs with fold change <2 and p value<0.05, were subjected to CLC analysis to perform clustering. n=1 sample for each cell type was included in the analysis.
B. Dot plot of marker genes for induced Treg, iPSC-Treg, primary CD4sp, primary Treg and primary CD4sp aligned to adult immune cells. For each gene, the average normalized expression (dot color) together with the percentage of cells expressing the gene (dot size) are shown for each cluster. Annotation based on Suo et al., 2022 [13]. *TRDC* was not found in the dataset as the iPSC cells were derived from TCR$\alpha\beta$ CD4+ cells and cloned.
C. Visualization of cells by cluster for iPSC-Tregs, cultured primary T conventional (Tconv), cultured primary Treg and induced Tregs using UMAPs.
D. scRNA-seq heatmap showing hierarchical clustering of a core Treg gene signature in iPSC-Tregs, iPSC-CD4sp, cultured primary Tregs, induced Tregs, and cultured primary Tconv.

FIGURE 5. Characterization of sorted and activated iPSC-CD4sp and iPSC-Tregs.

A

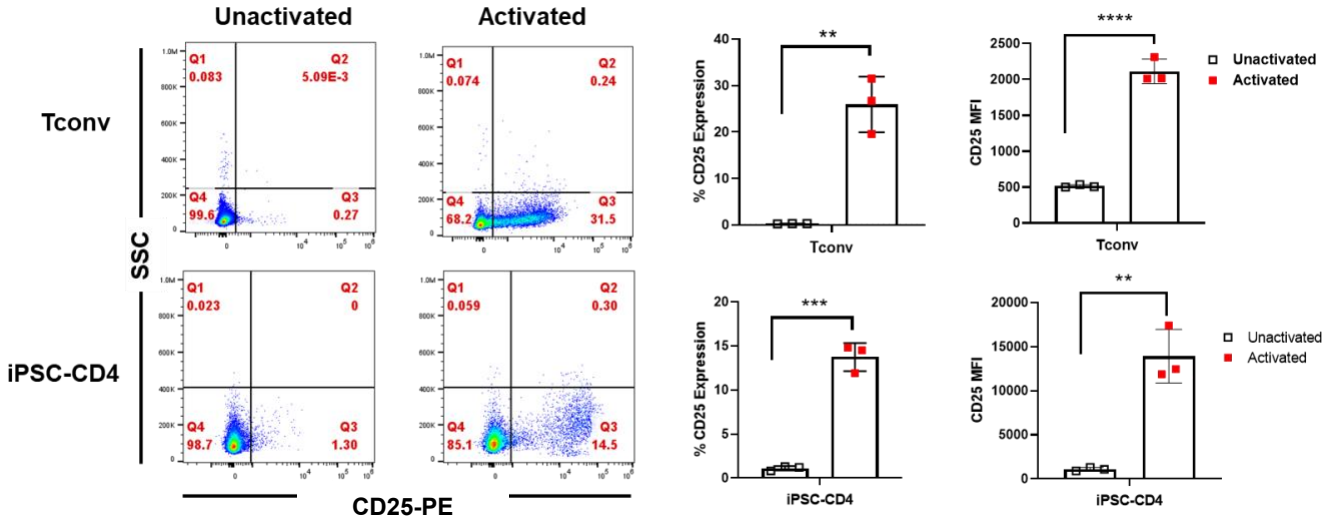

B

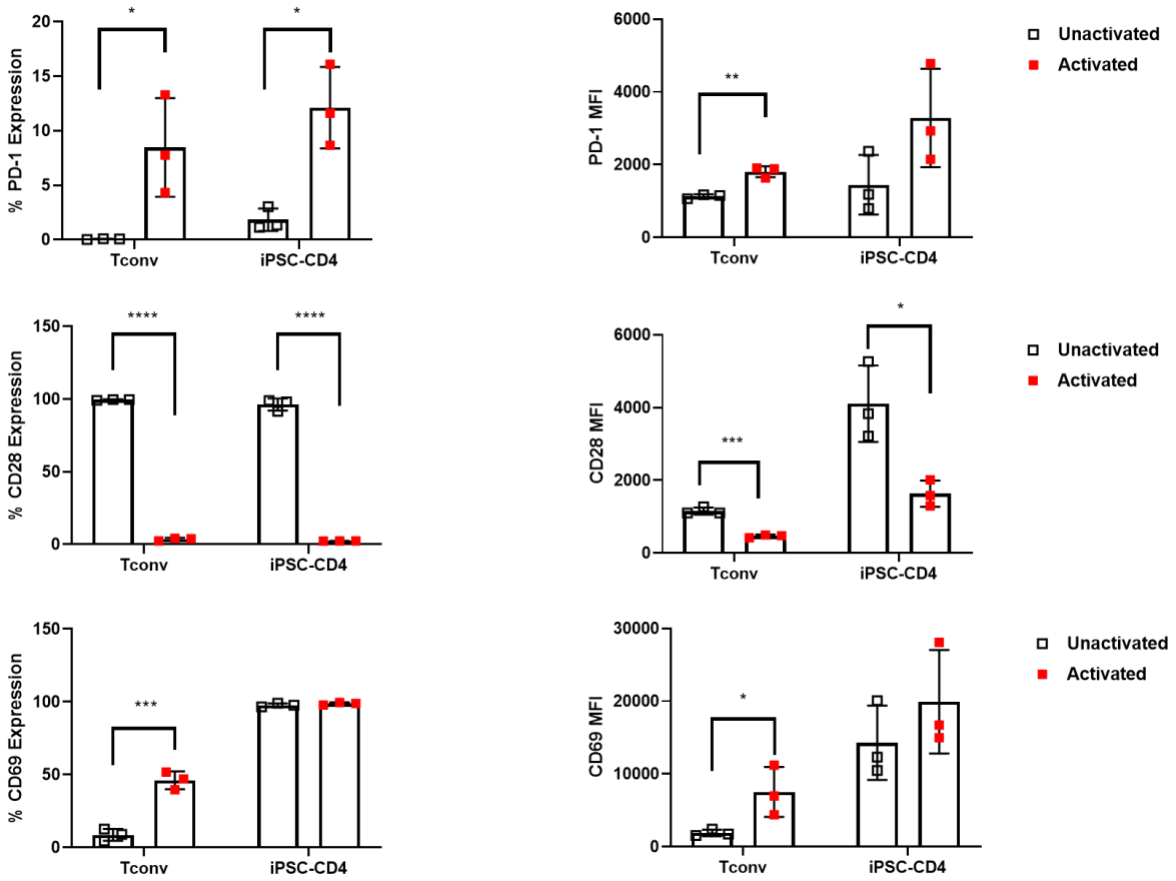

C

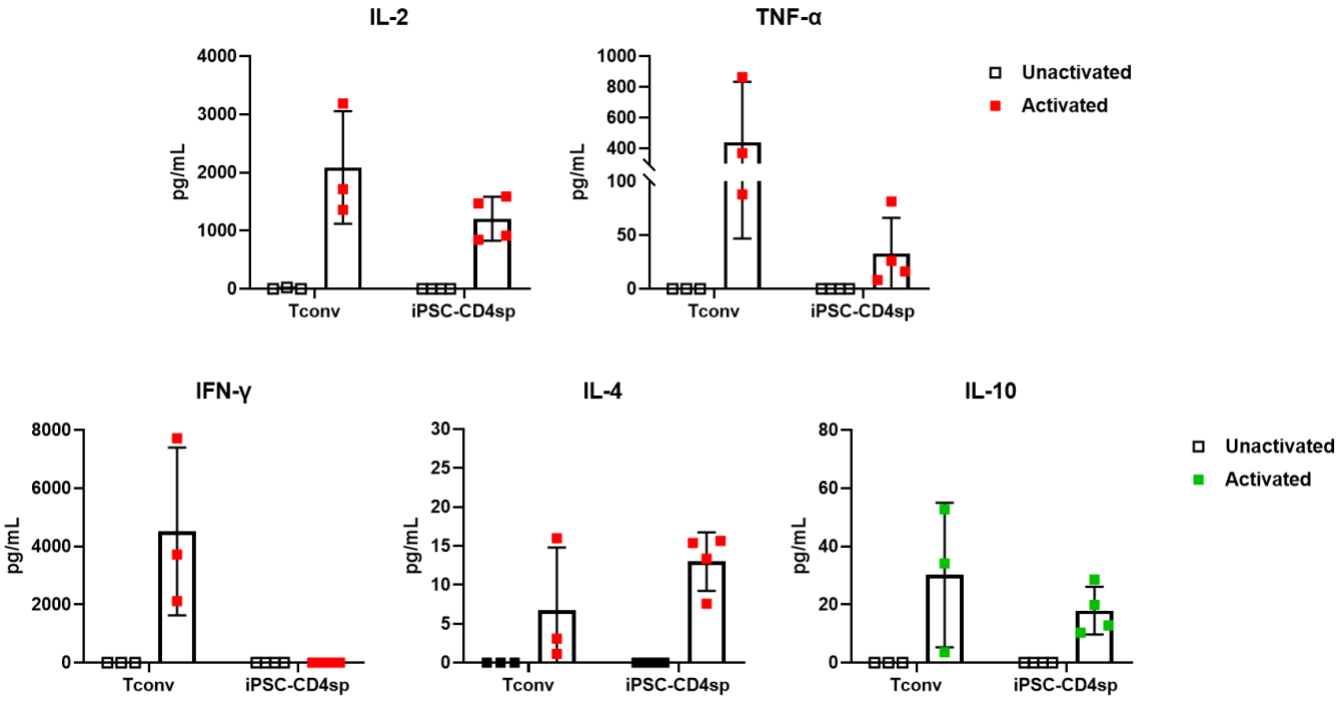
IL-2
TNF-α
IFN-γ
IL-4
IL-10
pg/mL
Tconv
iPSC-CD4sp
Unactivated
Activated

D

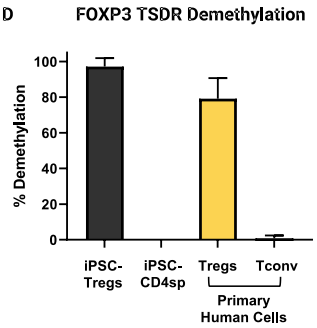
FOXP3 TSDR Demethylation
% Demethylation
iPSC-Tregs
iPSC-CD4sp
Tregs
Tconv
Primary Human Cells

E

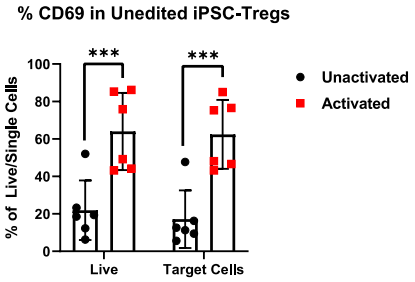
% CD69 in Unedited iPSC-Tregs
% of Live/Single Cells
***
***
Live
Target Cells
Unactivated
Activated

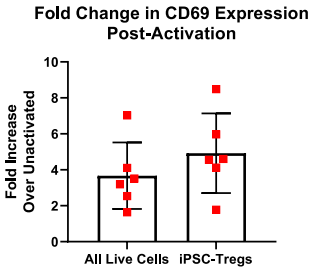
Fold Change in CD69 Expression Post-Activation
Fold Increase Over Unactivated
All Live Cells
iPSC-Tregs

F

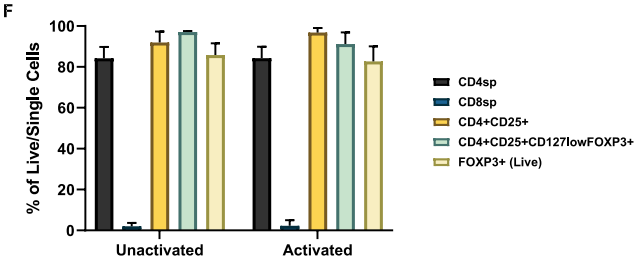
% of Live/Single Cells
Unactivated
Activated
CD4sp
CD8sp
CD4+CD25+
CD4+CD25+CD127lowFOXP3+
FOXP3+ (Live)

Figure 5. Characterization of sorted and activated iPSC-CD4sp and iPSC-Tregs.

A. Representative flow plots and expression of CD25 in sorted unactivated and activated iPSC-CD4sp T cells (n=1 clone) or T conventional (Tconv) cells (n=3) by flow cytometry after 48 hours. CD25 Median fluorescence intensity (MFI) was calculated (right).
B. Expression of activation markers (CD69, PD-1 and CD28) was assessed by flow cytometry after 48 hours of activation. MFI was calculated (right).
C. Secretion of cytokines from sorted unactivated and activated iPSC-CD4sp T cells 24 hours after activation (n=3, iPSC-CD4sp from n=1 clone; n=3, primary Tconv).
D. Assessment of FOXP3 TSDR demethylation in iPSC-Tregs, iPSC-CD4sp T cells, primary Tregs, and primary Tconv. Post-sort iPSC-Tregs were collected at day 57 for analysis and compared to primary controls (n=4, iPSC-Tregs; n=3, iPSC-CD4sp T cells, n=3, primary Tregs; n=3, primary Tconv).
E. Expression of CD69 in sorted unactivated and activated iPSC-Tregs. The expression of CD69 was assessed in both total live cell populations and target iPSC-Tregs by flow cytometry (left). Fold change in CD69 expression was assessed in activated total live and target iPSC-Tregs compared to unactivated total live cells and iPSC-Tregs (right, n=6 from n=3 clones, unactivated and activated).
F. Phenotype of unactivated and activated iPSC-Tregs. Treg markers were assessed by flow cytometric analysis (n=6 from n=3 clones).

Data represent mean ± SD of n independent experiments. P*<0.05, P**<0.01, P***<0.001, P****<0.0001 by unpaired two-tailed t-test.

Figure 6. Functional analysis of iPSC-Tregs.

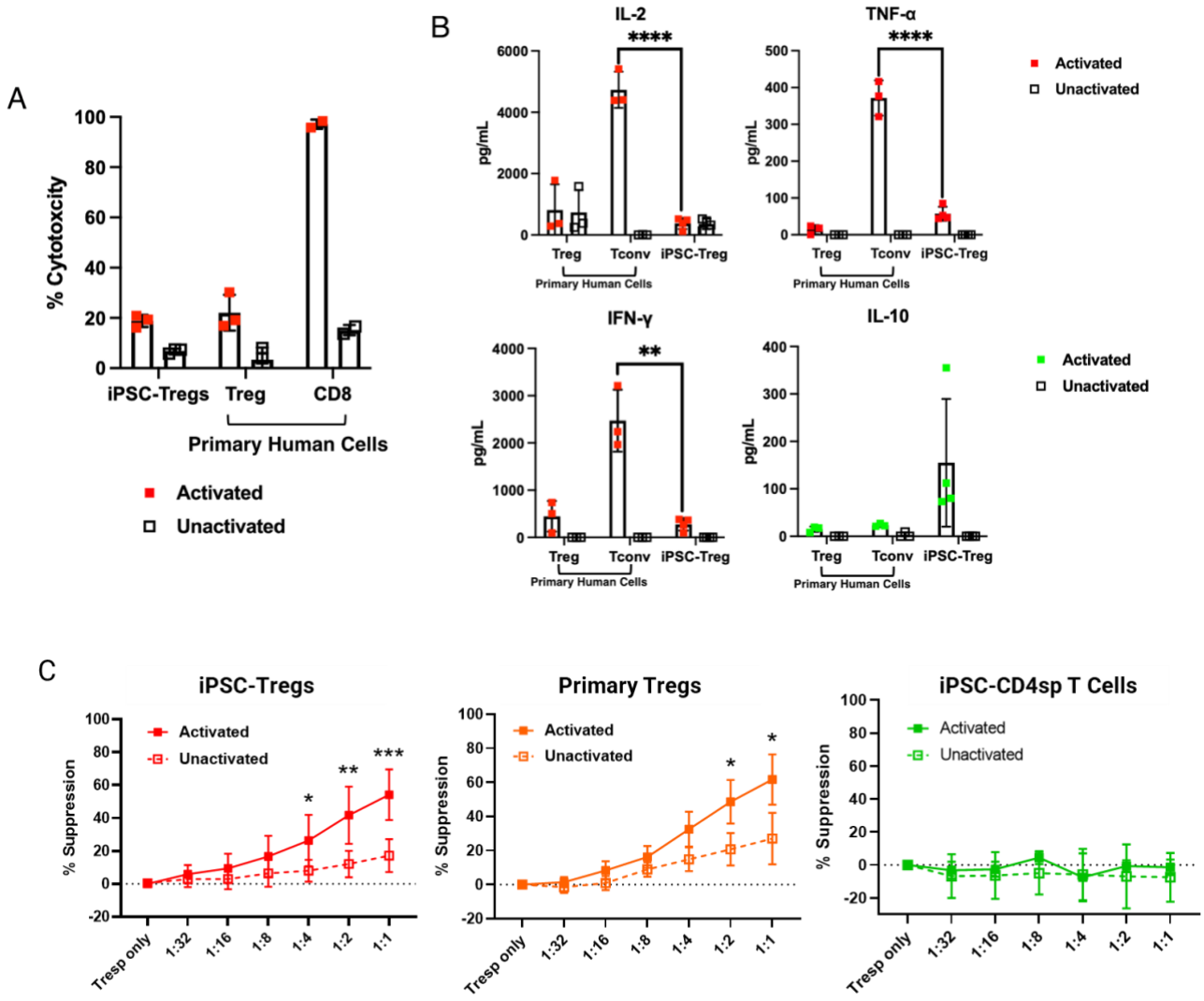

Figure 6. Functional analysis of iPSC-Tregs.

A. Cytotoxic activity of sorted unactivated and activated iPSC-Tregs as measured by an LDH release assay. iPSC-Tregs, primary Tregs, and primary CD8 T cells were cocultured with T conventional (Tconv) cells and LDH was measured after 3 days (n=3 from n=1 clone, iPSC-Tregs; n=3, primary Tregs; n=2, primary CD8 T cells).

B. Secretion of cytokines from sorted unactivated and activated iPSC-Tregs 24 hours after activation (n=4 from n=1 clone, iPSC-Tregs; n=3, primary Tregs; n=3, primary Tconv).

C. Suppression of Tconv proliferation by unactivated and activated iPSC-Tregs, iPSC-CD4sp T cells and primary Tregs. iPSC-Tregs, primary Tregs, and iPSC-CD4sp T cells were cocultured with activated CTV labeled Tconv and CTV dilution was measured by flow cytometry after 3 days (n=6 from n=3 clones, iPSC-Tregs; n=4, primary Tregs; n=3 from n=3 clones, iPSC-CD4sp).

Data represent mean ± SD of n independent experiments. P*<0.05, P**<0.01, P***<0.001 by unpaired two-tailed t-test.

FIGURE 7. Generation and Characterization of HLA-A2 CAR iPSC-Tregs

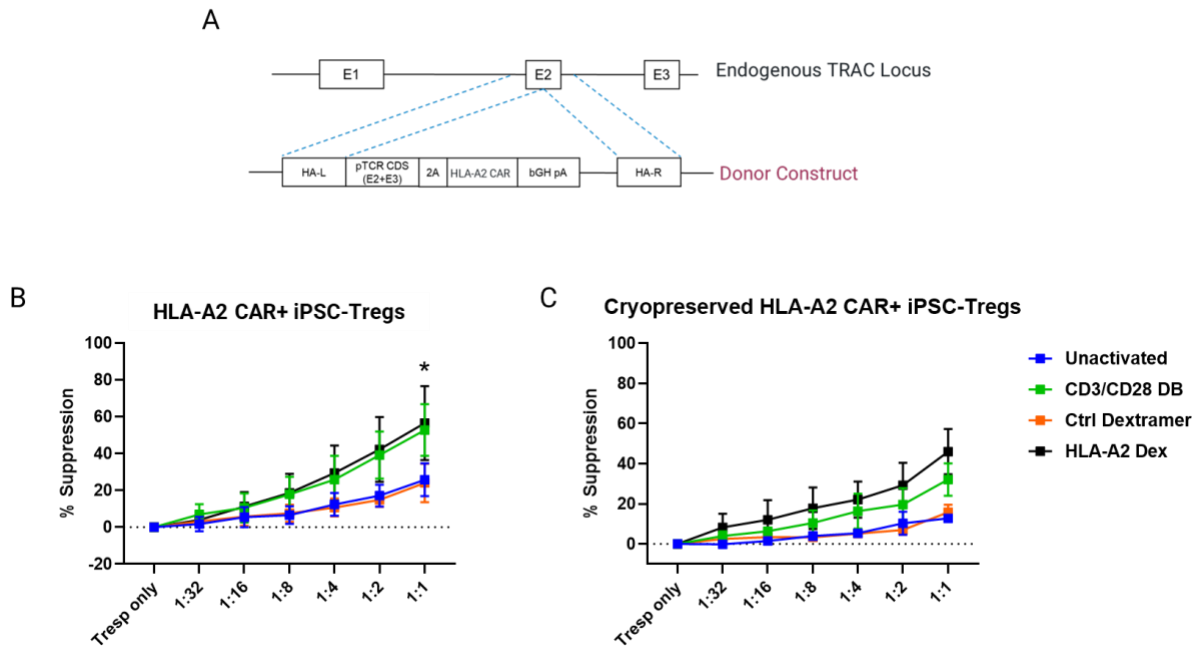

Figure 7. Generation and characterization of HLA-A2 CAR iPSC-Tregs.

A. Editing strategy for generation of HLA-A2 CAR iPSCs. A donor construct showing the TCR coding sequence and HLA-A2 CAR sequence flanked by homology arms targets exon 2 of the endogenous T Cell Receptor Alpha Constant (TRAC) locus.
B. Suppression of T conventional (Tconv) cell proliferation by HLA-A2 CAR+ iPSC-Tregs activated *via* the TCR or CAR. HLA-A2 CAR+ iPSC-Tregs were cocultured with activated CTV labeled Tconv and CTV dilution was measured by flow cytometry after 3 days (n=4 from n=2 clones). *$p<0.05$
C. Suppression of Tconv proliferation by cryopreserved HLA-A2 CAR+ iPSC-Tregs activated via the TCR or CAR. HLA-A2 CAR+ iPSC-Tregs were cocultured with activated CTV labeled Tconv and CTV dilution was measured by flow cytometry after 3 days (n=2 from n=2 clones).

Data represent mean ± SD of n independent experiments. P*<0.05 by unpaired two-tailed t-test.